

NOAA Technical Memorandum ERL ARL-109



ANALYTICAL SOLUTIONS OF A GRADIENT-TRANSFER MODEL
FOR PLUME DEPOSITION AND SEDIMENTATION

K. Shankar Rao

Atmospheric Turbulence and Diffusion Laboratory

Air Resources Laboratories
Silver Spring, Maryland
September 1981

noaa NATIONAL OCEANIC AND
ATMOSPHERIC ADMINISTRATION

Environmental Research
Laboratories

REPRODUCED BY
NATIONAL TECHNICAL
INFORMATION SERVICE
U.S. DEPARTMENT OF COMMERCE
SPRINGFIELD, VA. 22161

BIBLIOGRAPHIC DATA SHEET

| | | | | |
|--|--|----|---|--|
| 1. NOAA ACCESSION NUMBER NOAA-82042003 | | 2. | 3. RECIPIENT'S ACCESSION NUMBER P882 21515 B | |
| 4. TITLE AND SUBTITLE Analytical Solutions of a Gradient-Transfer Model for Plume Deposition and Sedimentation | | | 5. REPORT DATE Sept 1981 | |
| 7. AUTHOR(S) K. Shankar Rao (Atmospheric Turbulence and Diffusion Lab.) | | | 8. REPORT NO. NOAA-TM-ERL ARL-109 | |
| 9. PERFORMING ORGANIZATION NAME AND ADDRESS NOAA, Environmental Research Laboratories, Silver Spring, MD, 20902 Air Resources Laboratories | | | 10. PROJECT/TASK NO. | |
| 12. SPONSORING ORGANIZATION NAME AND ADDRESS Same | | | 11. CONTRACT/GRANT NO. Interagency Agreement AD-13-F-0177-0 | |
| | | | 13. TYPE OF REPORT AND PERIOD COVERED Tech. Memo. | |
| 15. PUBLICATION REFERENCE NOAA Technical Memorandum ERL ARL-109, September 1981. 84 p, 14 fig, 1 tab, 36 ref, 3 append. | | | | |
| 16. ABSTRACT This report reviews the methods available in the literature for including dry deposition in a Gaussian plume model. A gradient-transfer or K-theory model for the atmospheric transport and ground deposition of gaseous and particulate pollutants emitted from an elevated continuous point source is outlined. The analytical plume diffusion-deposition solutions are presented for various stability and mixing conditions. The deposition model has been applied to particulate pollutants with appreciable settling velocity and to gases which deposit on ground without settling. Calculated results of ground-level concentrations, vertical concentration profiles, surface deposition fluxes, and net deposition and suspension ratios are presented. The atmospheric stability and the magnitude of deposition velocity are shown to have significant effects on these results. The specification of gravitational settling and deposition velocities in the model is discussed. (Author modified) | | | | |
| 17. KEY WORDS AND DOCUMENT ANALYSIS | | | | |
| 17A. DESCRIPTORS | | | | |
| *Air pollution, *Diffusion, *Plumes, *Deposition, Pollutants, Reviews, Models | | | | |
| 17B. IDENTIFIERS/OPEN-ENDED TERMS | | | | |
| Atmospheric transport, Settling velocity, Gradient transfer | | | | |
| 17C. COSATI FIELD/GROUP | | | | |
| 4B, 13B | | | | |
| 18. AVAILABILITY STATEMENT Released for distribution: | | | 19. SECURITY CLASS (This report) UNCLASSIFIED | |
| <i>Ernie S. Downs</i> | | | 20. SECURITY CLASS (This report) UNCLASSIFIED | |

NOAA Technical Memorandum ERL ARL-109

ANALYTICAL SOLUTIONS OF A GRADIENT-TRANSFER MODEL
FOR PLUME DEPOSITION AND SEDIMENTATION

K. Shankar Rao

Atmospheric Turbulence and Diffusion Laboratory

Air Resources Laboratories
Silver Spring, Maryland
September 1981



UNITED STATES
DEPARTMENT OF COMMERCE

Malcolm Baldrige,
Secretary

NATIONAL OCEANIC AND
ATMOSPHERIC ADMINISTRATION

John V. Byrne,
Administrator

Environmental Research
Laboratories

George H. Ludwig
Director

NOTICE

Mention of a commercial company or product does not constitute an endorsement by NOAA Environmental Research Laboratories. Use for publicity or advertising purposes of information from this publication concerning proprietary products or the tests of such products is not authorized.

ATDL Contribution File No. 81/14

CONTENTS

| | |
|---|------|
| Figures | iv |
| Symbols and Abbreviations | vi |
| Acknowledgement | viii |
| Abstract | ix |
| 1. Introduction | 1 |
| 2. Review of Deposition Models | 3 |
| Source of depletion models | 4 |
| Surface depletion models | 6 |
| Partial reflection models | 7 |
| Gradient-transfer or K-theory models | 8 |
| 3. Gradient-Transfer or K-Theory Deposition Model..... | 12 |
| Mathematical formulation | 12 |
| Analytical solution | 14 |
| Concentration in terms of Gaussian dispersion parameters | 17 |
| Parameterization of concentration | 19 |
| Plume trapping | 22 |
| Well-mixed region | 24 |
| Surface deposition flux | 27 |
| Net deposition rate and suspension ratio | 28 |
| 4. Results and Discussion | 31 |
| Ground-level concentrations | 32 |
| Concentration profiles | 40 |
| Comparison with source depletion model | 43 |
| Surface deposition fluxes | 47 |
| Net deposition and suspension ratios | 50 |
| 5. Conclusions | 54 |
| References | 57 |
| Appendices | |
| A. Properties of error function and other relations | 60 |
| B. Settling and deposition velocities | 64 |
| C. Proposed field study | 68 |

FIGURES

| <u>Number</u> | | <u>Page</u> |
|---------------|--|-------------|
| 1 | Variation of plume-centerline GLC with downwind distance for different values of $V_d = W$ under slightly stable conditions | 33 |
| 2 | Variation of deposition effects on GLC for different values of wind speed | 34 |
| 3 | Variation of plume-centerline GLC with downwind distance for $V_d = W$ and $V_d > W$ under slightly unstable conditions | 36 |
| 4 | Variation of deposition effects on GLC for different unstable and neutral conditions | 37 |
| 5 | Variation of GLC of a gaseous pollutant ($W = 0$) for different values of the parameter V_d/U under slightly stable conditions .. | 38 |
| 6 | Variation of GLC of a particulate pollutant ($V_d = W$) for different values of the parameter V_d/U under slightly stable conditions | 39 |
| 7 | Deposition effects on vertical concentration profiles of a particulate pollutant under slightly stable conditions | 41 |
| 8 | Deposition effects on vertical concentration profiles of a particulate pollutant under extremely unstable conditions | 42 |
| 9 | Variation of GLC of a gaseous pollutant under slightly stable conditions: comparison to classical source depletion model prediction | 44 |
| 10 | Variation of GLC of a particulate pollutant under slightly stable conditions: comparison to tilted-plume source depletion model prediction | 46 |

| | | |
|-----|--|----|
| 11 | Variation of surface deposition flux of particles with downwind distance under stable conditions | 48 |
| 12 | Variation of surface deposition flux of particles with downwind distance under unstable and neutral conditions | 49 |
| 13 | Variation of net deposition and suspension ratios of particulate pollutant with downwind distance under stable conditions | 51 |
| 14 | Variation of net deposition and suspension ratios of particulate pollutant with downwind distance under unstable and neutral conditions | 52 |
| C-1 | Schematic representation of the effects of limited response of q and C sensors on power spectra, and of the effects of noise on the C-spectrum | 73 |

SYMBOLS AND ABBREVIATIONS

SYMBOLS

| | |
|------------|---|
| C | mean concentration of pollutant |
| C_{CWI} | crosswind-integrated concentration |
| D | surface deposition flux of pollutant |
| H | effective height of the source |
| K_y, K_z | eddy diffusivities in y and z directions |
| L | height of the inversion lid |
| L_y, L_z | length scales of concentration distribution in y and z directions |
| N | net deposition rate of pollutant |
| p,q | probability densities |
| Q | source strength or pollutant emission rate |
| U | mean wind speed |
| V_d | dry deposition velocity of pollutant |
| V_1 | $V_d - W/2$ |
| V_2 | $V_d - W$ |
| W | gravitational settling velocity of pollutant particles |
| x, y, z | horizontal downwind, horizontal crosswind, and vertical coordinates |

NONDIMENSIONAL QUANTITIES

| | |
|-------|------------------------------|
| g_1 | crosswind diffusion function |
|-------|------------------------------|

| | |
|-------------|--|
| g_2 | vertical diffusion function for stable conditions or unlimited mixing |
| g_2' | g_2 modified for deposition effects |
| g_3 | vertical diffusion function for unstable/neutral conditions, $\sigma_z < 1.6 L$ |
| g_3' | g_3 modified for deposition effects |
| g_4 | vertical diffusion function for unstable/neutral conditions, $\sigma_z \geq 1.6 L$ (well-mixed region) |
| g_4' | g_4 modified for deposition effects |
| \hat{H} | $H/\sqrt{2} \sigma_z$ |
| \hat{L} | $L/\sqrt{2} \sigma_z$ |
| \hat{V}_d | V_d/U |
| \hat{V}_1 | $\hat{V}_d - \hat{W}/2$ |
| \hat{V}_2 | $\hat{V}_d - \hat{W}$ |
| \hat{W} | W/U |
| \hat{x} | $x/\sqrt{2} \sigma_z$ |
| \hat{y} | $y/\sqrt{2} \sigma_y$ |
| \hat{z} | $z/\sqrt{2} \sigma_z$ |
| α_o | reflection coefficient |
| ζ | suspension ratio of pollutant |
| η | net deposition ratio of pollutant |

ABBREVIATIONS

| | |
|-----|-----------------------------------|
| EPA | Environmental Protection Agency |
| GLC | Ground-level concentration |
| KST | Atmospheric stability class index |
| P-G | Pasquill-Gifford |

ACKNOWLEDGEMENTS

This report was prepared for the Office of Research and Development, Environmental Sciences Research Laboratory of the U.S. Environmental Protection Agency to support the needs of EPA's Office of Toxic Substances. This work was accomplished under interagency agreements among the U.S. Department of Energy, the National Oceanic and Atmospheric Administration, and the EPA. The author is grateful to Dr. Jack Shreffler of ESRL for the opportunity to do this work, and for his interest and patience. The author also expresses his appreciation and thanks to the following members of the Atmospheric Turbulence and Diffusion Laboratory: Director Bruce Hicks for his understanding and support, and for contributing, at relatively short notice, his expertise to this report in Appendix C on the Proposed Field Study; Dr. Ray Hosker for the many discussions and suggestions and encouragement during the course of this work; Mrs. Ruth Green for arranging for computer, typing, and other assistance; Mr. Hal Snodgrass for writing the original graphics program and other computer assistance; Miss Lynne Satterfield for making the model test runs and plotting the results on computer; and Ms. Erma Yates for her expert technical typing and patient revisions.

ABSTRACT

This report reviews the methods available in the literature for including dry deposition in a Gaussian plume model. A gradient-transfer or K-theory model for the atmospheric transport and ground deposition of gaseous and particulate pollutants emitted from an elevated continuous point source is outlined. This analytical plume model treats gravitational settling and dry deposition in a physically realistic and more straightforward manner than other approaches. For practical application of the model, the eddy diffusivity coefficients in the analytical solutions are expressed in terms of the widely-used Gaussian plume dispersion parameters. The latter can be specified as functions of the downwind distance and the atmospheric stability class within the framework of the standard turbulence-typing schemes.

The analytical plume diffusion-deposition solutions are presented for various stability and mixing conditions. In the limit when settling and deposition velocities are zero, these equations reduce to the well-known Gaussian plume diffusion algorithms presently used in EPA models. Thus the analytical model for estimating deposition described here retains the ease of application associated with Gaussian plume models, and is subject to the same basic assumptions and limitations as the latter.

The deposition model has been applied to particulate pollutants with appreciable settling velocity and to gases which deposit on ground without settling. Calculated results of ground-level concentrations, vertical concentration profiles, surface deposition fluxes, and net deposition and suspension ratios are presented. The atmospheric stability and the magnitude of deposition velocity are shown to have significant effects on these results.

The specification of gravitational settling and deposition velocities in the model is discussed. A field study is proposed to measure one or more of the model parameters, and to provide a good data set for model validation over a 10 km distance from the source. The proposed field experiment is based on a modified Bowen ratio-turbulent variance approach, and it avoids the difficulties associated with the vertical gradient and eddy-correlation methods of surface flux measurements.

This report was submitted in partial fulfillment of Interagency Agreement No. AD-13-F-0177-0 by Atmospheric Turbulence and Diffusion Laboratory. This work, covering the period September 1980 to September 1981, was completed as of September 30, 1981.

SECTION 1

INTRODUCTION

Pollutant gases and suspended particles released into the atmosphere are transported by the wind, diffused and diluted by turbulence, and removed by several natural processes. An important removal mechanism is dry deposition of pollutants on the earth's surface by gravitational settling, eddy impaction, chemical absorption, and other effects. Depletion of airborne pollutant material in this manner affects its concentrations and residence time in the atmosphere. Moreover, acidic and toxic pollutants deposited on the ground may adversely impact on the local ecology, human health, biological life, structures, and ancient monuments. It is important, therefore, to obtain reliable estimates of dry deposition and its effects.

This report presents an analytical plume model for diffusion and dry deposition of gaseous and particulate pollutants from an elevated continuous point source, based on gradient-transfer or K-theory. The method essentially consists of solving the atmospheric advection-diffusion equation subject to a radiation boundary condition which equates the sum of the turbulent flux and the gravitational settling flux to the pollutant deposition flux at the surface. Though several analytical solutions of this problem are available in the air pollution

literature of the past two decades, the approach has not been widely used so far. This may be attributed to the complexity of the available solutions, and the usual difficulty in specifying the eddy diffusivity (K) coefficients under different atmospheric stability conditions.

In order to facilitate practical application of the model to air pollution problems, the K-coefficients are expressed in this report in terms of the widely used Gaussian plume dispersion parameters, which can be easily obtained from standard turbulence-typing schemes. The parameterized diffusion-deposition algorithms for various stability and mixing conditions are simplified and presented as analytical extensions of the well-known Gaussian plume diffusion algorithms presently used in EPA models. In the limit, when settling and deposition are zero, the new algorithms reduce to the Gaussian plume diffusion equations.

This report gives a brief review of the literature and existing methodologies of Gaussian diffusion-deposition models. Details of the formulation and solutions of the K-theory model are given, and the parameterized deposition algorithms are presented in such a way as to facilitate comparison with other available models. Calculated results of atmospheric concentrations, ground deposition fluxes, and net deposition and suspension ratios are presented and discussed. The specification of the settling and deposition velocities in the model is discussed, and a field study is proposed to determine one or more of these model parameters.

SECTION 2

REVIEW OF DEPOSITION MODELS

Most applied air pollution models are based on the Gaussian-plume formulation. These models have been extensively modified over the years to include pollutant removal mechanisms such as dry and wet deposition, and chemical transformation. An excellent review of air pollution deposition models, data requirements, and research needs is given by Hosker (1980). In this section, we briefly review Gaussian diffusion-deposition models by a comprehensive (though not all-inclusive) literature survey. Details of the mathematical formulations and results can be found in the literature cited.

Based on their theoretical approach, Gaussian plume diffusion-deposition models can be broadly classified as follows:

1. Source depletion models
2. Surface depletion models
3. Partial reflection models
4. Gradient-transfer or K-theory models

These models are discussed below for a continuous point source of strength Q located at $(x = 0, y = 0, z = H)$.

SOURCE DEPLETION MODELS

To account for dry deposition, Chamberlain (1953) introduced the concept of an "effective" source strength Q' , which depends on the amount of pollutant removed from the plume and, therefore, decreases with downwind distance x . The so-called source-depletion factor is given by

$$\frac{Q'(x)}{Q} = e^{-a \cdot I(x)}$$

where

$$a = \frac{V_d}{U}, \quad I(x) = \int_0^x \frac{dx'}{H'(x')}$$

$$H'(x) = \sqrt{\frac{\pi}{2}} \sigma_z \exp\left(\frac{H^2}{2\sigma_z^2}\right)$$

and V_d is the deposition velocity. Concentration at a receptor at x, y, z is now given by

$$C(x, y, z) = \frac{Q'(x)}{2\pi\sigma_y\sigma_z U} \exp\left(\frac{-y^2}{2\sigma_y^2}\right) \cdot \left[\exp\left\{\frac{-(z-H)^2}{2\sigma_z^2}\right\} + \exp\left\{\frac{-(z+H)^2}{2\sigma_z^2}\right\} \right]$$

Van der Hoven (1968) gave a good description of this method and graphical solutions of the source-depletion factors for several values of H under different stabilities. To account for gravitational settling of particles, the source depletion model can be combined with the "tilted plume" model (Csanady, 1958), where the plume slopes downward to compensate for the mean settling of the par-

ticles. This essentially involves replacing H by $H - Wx/U$, where W is the settling velocity, in the above equations.

Despite its popularity and wide use, which can be attributed to the simplicity of its formulations, the source depletion model is based on the physically unrealistic assumption that the shape of the concentration profile is unaltered by deposition, since material lost from the lower edge of the plume is evenly distributed through its entire depth. This assumption of instantaneous mixing is poor, especially under stable atmospheric conditions when the vertical eddy diffusivity K_z is small. Under these conditions, the source depletion model is known to overpredict the surface air concentrations and ground deposition flux at downwind locations close to the source, and to overestimate the total deposition between the source and the receptor (see, e.g., Horst, 1977). The largest errors appear for low sources in stable stratification over surfaces where relatively large deposition velocities occur.

The performance of the source-depletion model would be satisfactory for large K_z , since the concentration throughout the plume would then quickly adjust to ground-level removal of material by deposition. Taking $T_d = H'/V_d$ as the time scale for removal of material by deposition, and $T_k = H'^2/K_z$ as the time scale for the effect of deposition to diffuse through the plume, Prahm and Berkowicz (1978) emphasize that the condition

$$\frac{T_d}{T_k} = \frac{K_z}{V_d H'} > 1$$

should be satisfied for the source depletion model to be applicable (Fisher, 1979).

SURFACE DEPLETION MODELS

In the surface depletion models given by Horst (1974, 1977), the deposition flux to the surface is envisioned as due to material sinks (or negative sources), distributed continuously over the ground, which emit negative plumes that diffuse upward into the atmosphere. Superposition of the real plume and the integrated contributions of the distributed negative plumes yields the depleted plume concentration at receptor location (x,y,z) as

$$C(x,y,z) = Q \cdot R(x,y,z) - \int_{-\infty}^{\infty} \int_0^x V_d C(x',y',0) R(x-x',y-y',z) dx' dy',$$

where R is the relative concentration given by

$$R(x,y,z) = \frac{1}{2\pi\sigma_y\sigma_z U} \exp\left(\frac{-y^2}{2\sigma_y^2}\right) \left[\exp\left\{\frac{-(z-H)^2}{2\sigma_z^2}\right\} + \exp\left\{\frac{-(z+H)^2}{2\sigma_z^2}\right\} \right].$$

The calculation of the atmospheric concentration as described above is a tedious procedure since it involves the solution of a convolution integral of the areal source strength distribution with a point source relative concentration function. Numerical computations therefore take considerably more time than for the source depletion model. Horst (1976) also gave a simplified analytical procedure, and compared its results with those of the more complex computer model. Yamartino (1981) derived a formal solution for the crosswind-integrated form of the concentration in the surface depletion model, and gave practical representations of the solution for assumed exponential and power law forms of $\sigma_z(x)$, though these representations are only approximate in the latter case.

Horst (1979) has introduced a modified source depletion model which utilizes a factor to account for the dry deposition-induced change in vertical concentration distribution as a function of downwind distance. Though this method is easier to apply than the surface depletion model, their predictions differ close to the source in stable conditions. The original papers should be consulted for details.

Though the underlying concept is physically appealing, the surface depletion model has not been widely used so far, primarily due to its mathematical and computational complexities. Simplifications, such as those mentioned above, are aimed at reducing these difficulties and providing approximate solutions. It should be noted that the surface depletion model in its current form cannot be applied to cases where gravitational settling is important. Though the surface depletion model is a mathematically correct modification (for deposition) of the Gaussian plume model, it should be emphasized that the latter is only empirical, and not an exact solution of the diffusion problem.

PARTIAL REFLECTION MODELS

Baron et al. (1949) developed a dispersion model that includes both the real and the image source contributions, and suggested that the removal of airborne particles by deposition can be treated by adjusting the strength of the image source only. Csanady (1955) derived an analytic solution for this image source strength coefficient. In subsequent papers, Csanady (1957, 1958) recast his equations into Gaussian form. Overcamp (1976) extended Csanady's theory to

cover the case in which the settling velocity does not equal the deposition velocity, and gave an analytical expression for the concentration of gases and particulate pollutants as

$$C(x,y,z) = \frac{Q}{2\pi\sigma_y\sigma_z U} \exp\left(\frac{-y^2}{2\sigma_y^2}\right) \cdot \left[\exp\left\{\frac{-(z-H+Wx/U)^2}{2\sigma_z^2}\right\} + \alpha_o(x_G) \exp\left\{\frac{-(z+H-Wx/U)^2}{2\sigma_z^2}\right\} \right]$$

Here the reflection coefficient $\alpha_o(x_G)$ can be determined by solving an implicit relation for x_G , and an expression for $\alpha_o(x)$ which depends on W , V_d , U , H , and $\sigma_z(x)$. The latter equation was derived by setting the deposition flux equal to the difference in fluxes from the real and the image sources. Thus, in this model, the image source strength is adjusted to be a fraction α_o of the real source strength to account for deposition.

Overcamp (1976) showed that the partial reflection model predicts substantially lower values than the source depletion model for ground level concentration and deposition under stable conditions. Horst (1979) found that the partial reflection model is the easiest to use and, at short distances, is fairly close to his surface depletion model. Further downwind, however, the difference between the two models becomes quite large.

GRADIENT TRANSFER OR K-THEORY MODELS

The analytical gradient transfer model treats pollutant deposition in a

more physically realistic manner than the source depletion approach, and yet retains the ease of application associated with Gaussian plume dispersion models. Dry deposition is handled by taking both the gravitational settling flux and the ground deposition flux proportional to the local air concentration. In addition, this model uses other basic assumptions of the Gaussian plume model. The atmospheric transport equation is solved and analytical expressions are obtained for the atmospheric concentration and surface deposition flux. The theoretical formulations and concentration algorithms under various stability and mixing conditions are given in the next section.

Calder (1961) discussed the atmospheric diffusion of particulate material as a boundary value problem. He gave theoretical formulations in terms of the eddy diffusion coefficient, K_z , for the steady state two-dimensional problem of particulate material released from an elevated uniform crosswind line source. In particular, he suggested a radiation boundary condition to account for gravitational settling and deposition at the surface, and discussed its physics in relation to the diffusion of particles and gases.

Using the radiation boundary condition and the assumption that $K_z = \text{constant}$, Monin (1959) solved the problem of particulate diffusion from an instantaneous elevated point source of unit intensity. He gave exact analytical solutions for the crosswind integrated concentration and the normalized net deposition in terms of the normal integral probability functions.

Smith (1962) gave several analytical solutions to the problem of deposition of gases and particulate matter for steady state diffusion from a uniform crosswind line source. These solutions were based on a constant wind speed U , and

the eddy diffusivity coefficient specified by (a) $K_z = \text{constant}$, (b) $K_z = kz$, and (c) $K_z = k(L-z)$, where k is the von Kármán constant and L is the height of the inversion lid. Rounds (1955) solved this problem for an elevated line source with $V_d = W > 0$, $K_z = kz$, and a power law variation of U with z . Heines and Peters (1974) studied the diffusion of pollutants from an elevated point or line source, which are partially absorbed at the earth's surface. Their analytical solutions apply to the case when $W = 0$ and the diffusion coefficients are power functions of the downwind distance.

Scriven and Fisher (1975) gave an exact analytical solution for the crosswind integrated concentration from an elevated continuous point source, considering the dry deposition of the gaseous pollutant at the surface and its washout in rain. For $K_z \frac{\partial C}{\partial z} = 0$ at $z = L$ (representing the perfect reflection of material at the top of the boundary layer) and a constant K_z , the solution can be represented by the sum of a series whose terms involve the roots of a transcendental equation. In the limit when $L \rightarrow \infty$, the sum becomes an integral, and the solution reduces to the expressions given by Monin (1959) and Smith (1962).

Rao (1975) adapted these solutions to study the dispersion, deposition, and chemical transformation of the SO_2 plume from a power plant stack represented by an elevated continuous point source. In order to apply the analytical solutions, K_y and K_z were expressed in terms of the Gaussian dispersion parameters σ_y and σ_z . A constant first-order transformation rate of SO_2 to $\text{SO}_4^{=}$ was assumed. Concentrations of both species were calculated, and compared with observations at several downwind-receptors. Izrael, Mikhailova, and Pressman (1979) used Monin's instantaneous source solution to estimate the long-range transport of sulfur

dioxide and sulfates, assuming $K_z = \text{constant}$, $W = 0$, and non-equal $V_d > 0$ for the two species.

ErmaK (1977) solved the steady state atmospheric advection-diffusion equation for an elevated continuous point source, considering gravitational settling and deposition of the particles. The K-coefficients were expressed in terms of the corresponding $\sigma(x)$. ErmaK gave analytical expressions for the concentration and net deposition rate, and presented the results in non-dimensional form.

Following a similar approach, Rao and Satterfield (1980) calculated the atmospheric concentrations and surface deposition fluxes of fugitive dust emissions from a coal unloading facility. Assuming a lognormal probability of the particle size distribution, a mass spectrum was developed for six particle size ranges of the airborne coal fines, and each range was represented by its characteristic deposition and gravitational settling velocities in the model calculations.

No direct comparisons between the various analytical K-theory models and other deposition models are available. Based on the gradient-transfer theory, Berkowicz and Prahm (1978) described a pseudospectral two-dimensional numerical model, with height-dependent wind and eddy diffusivity profiles, for the dispersion and dry deposition of pollutants. They compared their results to the predictions of the conventional source depletion model as well as the analytical K-theory model for the case of constant wind and diffusivity.

SECTION 3

GRADIENT-TRANSFER OR K-THEORY DEPOSITION MODEL

In this section, the mathematical formulation of the K-theory for pollutant dispersion and deposition from an elevated continuous point source is given. The analytical solutions are expressed as extensions of the Gaussian plume algorithms (without deposition) currently used in EPA models. The non-reacting pollutant may be gaseous or suspended particulate matter. Level terrain is assumed.

MATHEMATICAL FORMULATION

We consider the steady state form of the atmospheric advection-diffusion equation:

$$U \frac{\partial C}{\partial x} = K_y \frac{\partial^2 C}{\partial y^2} + K_z \frac{\partial^2 C}{\partial z^2} + W \frac{\partial C}{\partial z} \quad (1)$$

Here, x , y , z are the horizontal downwind, horizontal crosswind, and vertical coordinates, respectively; U is the constant average wind speed, and W is the gravitational settling velocity (taken as positive in the downward negative z -direction) of the pollutant particles, C is the pollutant concentration at

(x, y, z) , and K_y and K_z are the eddy diffusivities in the crosswind and vertical directions, respectively.

For a continuous point source of strength Q located at $(x = 0, y = 0, z = H)$, the boundary conditions are given by

$$C(0, y, z) = Q/U \cdot \delta(y) \cdot \delta(z-H) \quad (2a)$$

$$C(\infty, y, z) = 0 \quad (2b)$$

$$C(x, \pm\infty, z) = 0 \quad (2c)$$

$$C(x, y, \infty) = 0 \quad (2d)$$

$$[K_z \cdot \partial C / \partial z + W \cdot C]_{z=0} = [V_d \cdot C]_{z=0} \quad (2e)$$

In Eq. (2a), which is the limiting form of the mass continuity equation at the source, δ is the Dirac-delta function such that $\int_{-\infty}^{\infty} \delta(y) dy \equiv 1$ when $y = 0$, and $\delta(y) \equiv 0$ when $y \neq 0$; $\int_{-\infty}^{\infty} \delta(z-H) dz \equiv 1$ when $z = H$, and $\delta(z-H) \equiv 0$ when $z \neq H$. Equation (2e) states that, at the ground-level, the sum of the turbulent transfer of pollutant down the concentration gradient and the downward settling flux due to the particles' weight is balanced by the net flux of material to the surface resulting from an exchange between the atmosphere and the surface; V_d is the deposition velocity which characterizes the interaction between the diffusing pollutant and the surface. For $V_d = 0$, the lower boundary acts as a perfect reflector of the pollutant; for $V_d = \infty$, it acts as a perfect sink; for the more

general case of $0 < V_d < \infty$, the pollutant reaching the earth's surface is partially retained and the rest reflected by it into the atmosphere. A so-called radiation boundary condition, which is analogous to Eq. (2e), commonly occurs in the theory of heat conduction.

The above formulations are general enough to be applicable to the calculation of dispersion and deposition of both gaseous and suspended particulate pollutants (see Appendix B). These formulations were discussed in detail by Calder (1961). For constant K_y and K_z (Fickian diffusion), the exact analytical solution of the problem was first given by Monin (1959), and later by Smith (1962), Scriven and Fisher (1975), Rao (1975), and Ermak (1977). These solutions due to various authors, though basically similar, differ somewhat due to different source conditions (instantaneous/continuous, line/point, elevated/ground-level), pollutant-species (gas/particles), and other assumptions used in their studies.

ANALYTICAL SOLUTION

The solution of Eqs. (1) and (2) can be expressed as

$$C(x, y, z) = \frac{Q}{U} \cdot p(x, y) \cdot q(x, z) \quad (3)$$

Substituting (3) in Eqs. (1) and (2) and using the separation of variables technique, two independent systems of equations and boundary conditions in p and q can be obtained. These equations can be solved using Laplace transform methods (Carslaw and Jaeger, 1959). The final solutions can be written as

$$p(x,y) = \frac{g_1(x,y)}{L_y} \quad (4a)$$

$$L_y = 2 \sqrt{\pi K_y x/U} \quad (4b)$$

$$g_1(x,y) = \exp\left\{-\frac{y^2}{4 K_y x/U}\right\} \quad (4c)$$

and

$$q(x,z) = \frac{g'_2(x,z)}{L_z} \quad (5a)$$

$$L_z = 2 \sqrt{\pi K_z x/U} \quad (5b)$$

$$g'_2(x,z) = \exp\left\{-\frac{W(z-H)}{2K_z} - \frac{W^2 x}{4K_z U}\right\} \cdot$$

$$\left[\exp\left\{\frac{-(z-H)^2 U}{4K_z x}\right\} + \exp\left\{\frac{-(z+H)^2 U}{4K_z x}\right\} \right] \quad (5c)$$

$$\cdot \frac{L_z V_1}{K_z} \exp\left\{\frac{V_1(z+H)}{K_z} + \frac{V_1^2 x}{K_z U}\right\} \cdot \operatorname{erfc}\left\{\frac{z+H+2V_1 x/U}{2\sqrt{K_z x/U}}\right\}$$

$$V_1 = V_d - W/2 \quad (5d)$$

In the above, the probability densities p and q are expressed in terms of g_1 and g'_2 to be consistent with notation presently used in the User's Guides for EPA models (see, e.g., Petersen, 1978; Pierce and Turner, 1980); $q(x,z)$ is the probability that a particle initially at $x = 0$ and $z = H$, the effective height of the source, will be at z after travelling a distance x . In the trivial deposition case of $W = 0$ and $V_d = 0$, $g'_2 \equiv g_2$, which is given by

$$g_2(x,z) = \exp\left\{\frac{-(z-H)^2 U}{4K_z x}\right\} + \exp\left\{\frac{-(z+H)^2 U}{4K_z x}\right\} \quad (6)$$

The crosswind-integrated concentration at distance x from the continuous point source Q is given by

$$C_{CWI} = \bar{C}(x,z) = \frac{Q}{U} q(x,z) = \frac{Q}{UL_z} g'_2(x,z) \quad (7)$$

Alternately, $\bar{C}(x,z)$ can be interpreted as the concentration at (x,z) from a uniform crosswind line source of strength Q located at $(0,H)$. For $W = 0$ (no gravitational settling) and $H = 0$ (ground-level source), the uniform crosswind line source solution from Eqs. (5) and (7) agrees with the corresponding expression given by Smith (1962). The expression for $q(x,z)$ from Eq. (5) is consistent with the corresponding solution for instantaneous point source given by Monin (1959), except that the dimensionless grouping $L_z V_1 / K_z$ in Eq. (5c) was incorrectly shown as $L_z K_z / V_1$ in that paper. Some useful properties and relations of the complementary error function in Eq. (5c) are given in Appendix A.

Equations (4) and (5) show that only the vertical diffusion field is modified by deposition. For $W = 0$, the first part of Eq. (5c) gives the familiar solution with zero deposition, and the second part is the modification representing the loss due to deposition. For values of V_d of the order of a few centimeters per second, the shape of the vertical concentration profile is modified only slightly. The vertical concentration gradient becomes slightly positive near the ground although, as pointed out by Smith (1962), this is not easy to measure in the field.

CONCENTRATION IN TERMS OF GAUSSIAN DISPERSION PARAMETERS

In order to facilitate the practical application of the analytical solutions, the eddy diffusivities K_y and K_z are expressed here in terms of σ_y and σ_z , the standard deviations of the crosswind and vertical Gaussian concentration distributions, respectively, as follows:

$$K_y = \frac{U}{2} \frac{d\sigma_y^2}{dx}, \quad K_z = \frac{U}{2} \frac{d\sigma_z^2}{dx} \quad (8)$$

Thus, for Fickian diffusion, K_y and K_z can be expressed by the relations

$$K_y = \sigma_y^2 \cdot U/2x, \quad K_z = \sigma_z^2 \cdot U/2x, \quad (9)$$

in order to utilize the vast amount of empirical data on the Gaussian plume parameters σ_y and σ_z available in the literature for a variety of meteorological and terrain conditions. An excellent review and summary of these data can be found in Gifford (1976). Equation (9), in combination with the Gaussian assumption (see, e.g., Gifford, 1968), forms the basis for the practical plume diffusion formulas that are found in the literature on applications.

Utilizing Eq. (9), one can describe the modified Gaussian plume which results in the general case when gravitational settling and deposition are included. The general solution for a continuous point source given by Eqs. (3) to (5) can be now written as

$$C(x,y,z) = \frac{Q}{U} \cdot \frac{g_1}{L_y} \cdot \frac{g_2}{L_z} \quad (10a)$$

$$g_1(x,y) = \exp(-y^2/2\sigma_y^2), \quad L_y = \sqrt{2\pi} \sigma_y \quad (10b)$$

$$g_2'(x,z) = \exp\left\{\frac{-W(z-H)r}{2\sigma_z} - \frac{W^2 r^2}{8}\right\}.$$

$$\left[\exp\left\{\frac{-(z-H)^2}{2\sigma_z^2}\right\} + \exp\left\{\frac{-(z+H)^2}{2\sigma_z^2}\right\} \right] \quad (10c)$$

$$- \sqrt{2\pi} V_1 r \cdot \exp\left\{\frac{V_1 r(z+H)}{\sigma_z} + \frac{V_1^2 r^2}{2}\right\} \cdot \operatorname{erfc}\left\{\frac{z+H}{\sqrt{2}\sigma_z} + \frac{V_1 r}{\sqrt{2}}\right\} \Big]$$

$$L_z = \sqrt{2\pi} \sigma_z, \quad V_1 = V_d - W/2 \quad (10d)$$

$$r = \sigma_z/K_z = 2x/U\sigma_z \quad (10e)$$

The above analytical expression for concentration, based on an exact solution for constant diffusion coefficients, is only approximate, since the K's are expressed in terms of the empirical Gaussian dispersion parameters. Equation (10) agrees with the corresponding expressions given by Rao (1975) and Ermak (1977), except for the errors in the latter reference in the argument of the last exponential function in Eq. (10c). This equation can be further simplified by noting

$$\frac{V_1 r(z+H)}{\sigma_z} + \frac{V_1^2 r^2}{2} = \xi^2 - \frac{(z+H)^2}{2\sigma_z^2}, \quad (11a)$$

where

$$\xi = \frac{z+H}{\sqrt{2}\sigma_z} + \frac{V_1 r}{\sqrt{2}} \quad (11b)$$

Using (11) and noting that $e^{a-b} = e^a \cdot e^{-b}$, Eq. (10c) can be now written as

$$g_2'(x, z) = \exp \left\{ \frac{-W(z-H)r}{2\sigma_z} - \frac{W^2 r^2}{8} \right\} \cdot \left[\exp \left\{ \frac{-(z-H)^2}{2\sigma_z^2} \right\} + \exp \left\{ \frac{-(z+H)^2}{2\sigma_z^2} \right\} \cdot \left(1 - \sqrt{2\pi} v_d r e^{\xi^2} \operatorname{erfc} \xi \right) \right] \quad (12)$$

This equation agrees with the corresponding expression for an instantaneous source given by Izrael, Mikhailova, and Pressman (1979), except for the argument of the first exponential term, which they wrongly give as $\{W H r / 2 \sigma_z - W^2 r^2 / 2\}$. For $W = 0$ in Eq. (12), the effect of deposition can be seen as a multiplication of the image-source or reflection term, $\exp\{-(z+H)^2 / 2 \sigma_z^2\}$, by a factor $\alpha = 1 - \sqrt{2\pi} v_d r e^{\xi^2} \operatorname{erfc} \xi$, where $-1 \leq \alpha \leq 1$. A similar modification of the reflection term, multiplying it by a factor $\alpha(x, z)$, is done in the so-called partial-reflection model (Csanady, 1955; Overcamp, 1976) to account for deposition effects, though the value of $\alpha(x, z)$ is determined in that model from an implicit equation based on considerations of the streamlines from the real and image sources and other physical arguments. It can be easily checked that Eq. (12) satisfies the equivalent of the deposition boundary condition (2e) given by

$$\left[\frac{\sigma_z}{r} \frac{\partial g_2'}{\partial z} + W g_2' \right]_{z=0} = \left[v_d g_2' \right]_{z=0} \quad (13)$$

PARAMETERIZATION OF CONCENTRATION

In order to parameterize the expressions for concentration under various stability conditions, and to considerably reduce the difficulty in typing the equations, we adopt the following nondimensionalization scheme: All velocities

are nondimensionalized by U ; the constant mean wind speed. The horizontal downwind distance x and all vertical height quantities are nondimensionalized by $\sqrt{2} \sigma_z$. The horizontal crosswind distance y is nondimensionalized by $\sqrt{2} \sigma_y$. Thus, we define

$$\begin{aligned}\hat{W} &= W/U, \quad \hat{V}_d = V_d/U \\ \hat{V}_1 &= \hat{V}_d - \hat{W}/2 = V_1/U \\ \hat{V}_2 &= \hat{V}_d - \hat{W} = V_2/U \\ \hat{x} &= x/\sqrt{2} \sigma_z, \quad \hat{z} = z/\sqrt{2} \sigma_z \\ \hat{H} &= H/\sqrt{2} \sigma_z, \quad \hat{L} = L/\sqrt{2} \sigma_z \\ \hat{y} &= y/\sqrt{2} \sigma_y\end{aligned}\tag{14}$$

where the capped quantities denote the nondimensionalized variables, and L is the mixing height. The concentration from Eqs. (10) and (12) can be now written as

$$C(\hat{x}, \hat{y}, \hat{z}) = \frac{Q}{U} \cdot \frac{g_1}{L_y} \cdot \frac{g_2'}{L_z}\tag{15a}$$

$$g_1(\hat{x}, \hat{y}) = \exp(-\hat{y}^2)\tag{15b}$$

$$\begin{aligned}g_2'(\hat{x}, \hat{z}) &= \exp\left\{-2\hat{W}(\hat{z}-\hat{H})\hat{x} - \hat{W}^2\hat{x}^2\right\} \cdot \\ &\left[\exp\left\{-(\hat{z}-\hat{H})^2\right\} + \exp\left\{-(\hat{z}+\hat{H})^2\right\} \right] \cdot \\ &\left(1 - 4\sqrt{\pi} \hat{V}_1 \hat{x} e^{\xi^2} \operatorname{erfc} \xi \right)\end{aligned}\tag{15c}$$

where

$$\xi = \hat{z} + \hat{H} + 2 \hat{V}_1 \hat{x} ,$$

$$L_y = \sqrt{2\pi} \sigma_y , L_z = \sqrt{2\pi} \sigma_z . \quad (15d)$$

Equation (15c) clearly shows that concentration depends on the ratios W/U and V_d/U , not on W and V_d per se. Thus, the effect on concentration of large values of W and V_d at high wind speeds is the same as that of small values of W and V_d at low wind speeds, provided W/U and V_d/U remain constant.

From Eq. (15), the ground-level ($\hat{z} = 0$) centerline ($\hat{y} = 0$) concentration is given by

$$C(\hat{x}, 0, 0) = \frac{Q}{\pi \sigma_y \sigma_z U} \cdot \exp \left\{ 2 \hat{W} \hat{H} \hat{x} - \hat{W}^2 \hat{x}^2 - \hat{H}^2 \right\} \cdot \left[1 - 2 \sqrt{\pi} \hat{V}_1 \hat{x} e^{\xi^2} \operatorname{erfc} \xi \right] \quad (16)$$

where $\xi = \hat{H} + 2 \hat{V}_1 \hat{x}$. Further simplifications are possible for gases or small particles ($\hat{W} = 0$, $\hat{V}_1 = \hat{V}_d$) or ground-level sources ($\hat{H} = 0$). In the trivial deposition case ($\hat{W} = 0$ and $\hat{V}_d = 0$), $g'_2 = g_2$ and Eq. (15) reduces to the well-known Gaussian plume model.

Equations (15) and (16) are applicable in EPA models to the stable atmosphere (P-G stability classes E and F) or for the case of an unstable or neutral atmosphere with unlimited mixing ($L > 5000$ m).

PLUME TRAPPING

Following the current practice in EPA models (e.g., Petersen, 1978; Pierce and Turner, 1980), for unstable or neutral atmosphere (P-G stability classes A to D), the mixing depth or the height of the inversion lid L should be included in the algorithms. This is usually done through calculation of multiple eddy reflections (Turner, 1970) from both the ground and the stable layer aloft, when the plume is trapped between these two surfaces.

In the general case when settling and deposition effects are considered, the expressions for concentration under plume trapping conditions can be written directly from Eq. (15) as follows:

$$C(\hat{x}, \hat{y}, \hat{z}) = \frac{Q}{U} \cdot \frac{g_1}{L_y} \cdot \frac{g_3'}{L_z} \quad (17a)$$

$$g_1(\hat{x}, \hat{y}) = \exp(-\hat{y}^2) \quad (17b)$$

$$g_3'(\hat{x}, \hat{z}) = \sum_{N=-\infty}^{\infty} \left[\exp\left\{-2\hat{W}(\hat{z}-\hat{H}_1)\hat{x} - \hat{W}^2\hat{x}^2\right\} \cdot \left[\exp\left\{-(\hat{z}-\hat{H}_1)^2\right\} + \exp\left\{-(\hat{z}+\hat{H}_1)^2\right\} \cdot \left(1-4\sqrt{\pi} \hat{V}_1 \hat{x} e^{\xi_1^2} \operatorname{erfc} \xi_1\right) \right] \right] \quad (17c)$$

where

$$\xi_1 = \hat{z} + \hat{H}_1 + 2 \hat{V}_1 \hat{x} ,$$

$$\hat{H}_1 = \hat{H} + 2 N \hat{L} , \quad (17d)$$

$$L_y = \sqrt{2\pi} \sigma_y , \quad L_z = \sqrt{2\pi} \sigma_z .$$

Equation (17c), which gives a zero mass flux condition at $z = L$, follows directly from Eq. (15c) by replacing \hat{H} with $\hat{H}_1 = \hat{H} + 2NL$, and summing over N from $-\infty$ to ∞ . Thus, g_3' consists of the sum of an infinite number of terms, each of them similar to g_2' but with a different effective height \hat{H}_1 ; each one of these terms independently satisfies the diffusion equation (1) and the boundary conditions, Eq. (2). Therefore, the sum of these independent solutions (i.e., g_3') also satisfies the governing equations.

An important test for the solution g_3' is its rapid convergence to a limit as $N \rightarrow \pm \infty$. Expanding Eq. (17c) following Turner (1970; p.36) and noting the behavior of $e^{\xi^2} \cdot \text{erfc } \xi$ (Appendix A) for large positive and negative values of ξ , one can see that $g_3'(\hat{x}, \hat{z})$ converges rapidly to a limit. Tests showed that a maximum of $N = \pm 10$ eddy reflections are adequate to obtain convergence of the sum within the specified tolerance of 0.01.

Another test of algorithm (17c) is that g_3' should reduce to g_3 in the limit of $\hat{W} = 0$ and $\hat{V}_d = 0$. For this trivial deposition case, Eq. (17c) reduces to

$$g_3'(\hat{x}, \hat{z}) = \sum_{N=-\infty}^{\infty} \left[\exp\left\{-\left(\hat{z} - \hat{H} - 2NL\right)^2\right\} + \exp\left\{-\left(\hat{z} + \hat{H} + 2NL\right)^2\right\} \right] \quad (18a)$$

The expression for g_3 currently used in EPA models (e.g., Petersen, 1978; Pierce and Turner, 1980) without deposition effects is

$$g_3(\hat{x}, \hat{z}) = \sum_{N=-\infty}^{\infty} \left[\exp\left\{-\left(\hat{z} - \hat{H} + 2NL\right)^2\right\} + \exp\left\{-\left(\hat{z} + \hat{H} + 2NL\right)^2\right\} \right] \quad (18b)$$

Despite the differences in sign within the arguments of the first exponential function, Eqs. (18a) and (18b) are identical. This can be verified by expanding the right hand sides of both equations following Turner (1970), which shows that g_3' and g_3 represent sums of identical terms, though the sequence in which these terms appear in the sums may be different in the two cases.

From Eq. (17), the ground-level ($\hat{z} = 0$) centerline ($\hat{y} = 0$) concentration is given by

$$C(\hat{x}, 0, 0) = \frac{Q}{\pi \sigma_y \sigma_z U} \cdot \sum_{N=-\infty}^{\infty} \left[\exp \left\{ 2\hat{W} \hat{H}_1 \hat{x} - \hat{W}^2 \hat{x}^2 - \hat{H}_1^2 \right\} \cdot \left(1 - 2\sqrt{\pi} \hat{V}_1 \hat{x} e^{\xi_1^2} \operatorname{erfc} \xi_1 \right) \right], \quad (19)$$

where $\xi_1 = \hat{H}_1 + 2 \hat{V}_1 \hat{x}$, and $\hat{H}_1 = \hat{H} + 2 N \hat{L}$.

Further simplification is possible for gases or small suspended particles ($\hat{W} = 0$, $\hat{V}_1 = \hat{V}_d$) or ground-level sources ($\hat{H} = 0$, $\hat{H}_1 = 2 N \hat{L}$).

Equations (17) and (19) are applicable to the unstable or neutral atmosphere when $\sigma_z < 1.6 L$, according to the current practice in EPA models.

WELL-MIXED REGION

For $\sigma_z \geq 1.6 L$, for unstable or neutral cases, the pollutant is assumed to be well-mixed by atmospheric turbulence, resulting in a uniform vertical concentration profile. This concentration is independent of the source height

(\hat{H} or \hat{H}_1) as well as the receptor height (\hat{z}) due to the repeated eddy reflections from the ground and the stable layer aloft at $z = L$. Therefore, we can calculate this uniform concentration as the average value in a layer of thickness L , setting $H=0$ in Eq. (15) or $H_1=0$ in Eq. (17), as follows:

$$C(\hat{x}, \hat{y}, \hat{z}) = \frac{Q}{U} \cdot \frac{g_1}{L_y} \cdot \frac{g_4'}{L} \quad (20a)$$

$$g_1(\hat{x}, \hat{y}) = \exp(-\hat{y}^2) \quad (20b)$$

$$g_4'(\hat{x}) = \int_0^{\infty} \left[\frac{g_3'}{L_z} \right]_{H_1=0}^{\hat{z}} d\hat{z} \equiv \int_0^{\infty} \left[\frac{g_2'}{L_z} \right]_{H=0}^{\hat{z}} d\hat{z} \quad (20c)$$

Carrying out the integration using the relations given in Appendix A, we obtain the following algorithms:

For $\hat{V}_d \neq \hat{W}$ or $\hat{V}_2 = (\hat{V}_d - \hat{W}) \neq 0$,

$$g_4'(\hat{x}) = (\hat{V}_1/\hat{V}_2) \cdot \exp(4 \hat{V}_d \hat{V}_2 \hat{x}^2) \cdot \operatorname{erfc}(2 \hat{V}_1 \hat{x}) - (\hat{W}/2\hat{V}_2) \cdot \operatorname{erfc}(\hat{W} \hat{x}) \quad (20d)$$

For $\hat{V}_d = \hat{W}$ or $\hat{V}_2 = 0$,

$$g_4'(\hat{x}) = (1 + 2 \hat{x}_1^2) \operatorname{erfc} \hat{x}_1 - (2\hat{x}_1/\sqrt{\pi}) \exp(-\hat{x}_1^2) \quad (20e)$$

where $\hat{x}_1 = \hat{V}_d \hat{x}$.

In the limit of $\hat{V}_d = \hat{W} = 0$, Eq. (20e) reduces to

$$g_4' = 1 = g_4 \quad (21)$$

as in present EPA models without deposition effects.

The selection of $\sigma_z = 1.6 L$ as the transition from Eq. (17) to Eq. (20) for the well-mixed region is obviously based on sensitivity tests which indicated that, for all H and z between the ground and the mixing height, the vertical distribution of concentration is uniform with height when $\sigma_z > 1.6L$. Though this value is nearly twice as large as the recommended values of Pasquill (1976) and the AMS Workshop (Hanna et al., 1977), it allows for a smooth transition to a uniform vertical concentration profile for receptors above the ground ($z > 0$), and for effective heights of emission approaching the mixing height (Pierce and Turner, 1980). Since EPA models usually limit maximum σ_z to 5000 m, we can derive $L_{\max} < (\sigma_z)_{\max} / 1.6 = 3125$ m as the upper limit for the value of the mixing depth which allows one to use the well-mixed region concentration algorithms.

A summary of the applicable concentration algorithms for various stability and mixing conditions is shown in Table 1. All the new algorithms reduce to the current EPA algorithms in the limit when settling and deposition velocities are zero.

TABLE 1

SUMMARY OF CONCENTRATION ALGORITHMS WITH SETTLING AND DEPOSITION EFFECTS

| Stability & Mixing Conditions | Applicable Concentration Algorithms & Equation Numbers |
|---|--|
| 1. Stable conditions or unlimited mixing ($\sigma_z > 5000$ m) | $C(\hat{x}, \hat{y}, \hat{z}) = \frac{Q}{U} \cdot \frac{g_1}{L_y} \cdot \frac{g_2'}{L_z}$ EQ. (15) |
| 2. Unstable/neutral, non-uniform mixing ($\sigma_z < 1.6L$) | $C(\hat{x}, \hat{y}, \hat{z}) = \frac{Q}{U} \cdot \frac{g_1}{L_y} \cdot \frac{g_3'}{L_z}$ EQ. (17) |
| 3. Unstable/neutral, well-mixed region ($\sigma_z \geq 1.6L$ and $\sigma_z \leq 5000$ m) | $C(\hat{x}, \hat{y}, \hat{z}) = \frac{Q}{U} \cdot \frac{g_1}{L_y} \cdot \frac{g_4'}{L}$ EQ. (20) |

SURFACE DEPOSITION FLUX

The surface deposition flux at ground-level receptors is calculated directly from Eq. (2e) as

$$D(\hat{x}, \hat{y}) = v_d \cdot C(\hat{x}, \hat{y}, 0) \quad (22)$$

This is the amount of pollutant deposited per unit time per unit surface area. D is usually calculated as $\text{kg}/\text{km}^2\text{-hr}$, while seasonal estimates are expressed as

kg/km²-month. The estimation of the monthly or yearly surface deposition fluxes at a given downwind distance x from the source in a given wind-directional sector requires the knowledge of the fraction of the time that a mean wind of a given magnitude blows in that direction in a month or a year, respectively. To obtain D in kg/km²-hr when V_d is given in cm/s and C in g/m³, the right-hand side of Eq. (22) should be multiplied by 36000. For D calculations, the ground-level receptor is generally defined as any receptor which is not higher than 1 meter above the local ground-level elevation.

NET DEPOSITION RATE AND SUSPENSION RATIO

The net deposition rate, $N(\hat{x})$, which is the total amount of pollutant deposited per unit time between the source and the downwind distance \hat{x} , can be calculated from

$$N(\hat{x}) = \int_0^{\hat{x}} \int_{-\infty}^{\infty} D(\hat{x}', \hat{y}) d\hat{y} d\hat{x}' \quad (23)$$

where D is the surface deposition flux from Eq. (22). N is usually calculated as kg/hr, while seasonal estimates of N are expressed as kg/month.

The calculation of $N(\hat{x})$ from Eq. (23) presents considerable difficulty. A simpler alternate approach is derived by appealing to the mass continuity condition. The total amount of pollutant released per unit time is given by the source emission rate Q . We define ζ as the proportion (fraction) of this pollutant

released at $(0,0,\hat{H})$ that still remains airborne at downwind distance \hat{x} . Then, the proportion (fraction) η of the total pollutant deposited on the earth's surface over distance \hat{x} is given by

$$\eta(\hat{x}) = \frac{N(\hat{x})}{Q} = 1 - \zeta(\hat{x}) \quad (24)$$

$$\zeta(\hat{x}) = \int_0^{\infty} q(\hat{x}, \hat{z}) \, d\hat{z} = \int_0^{\infty} \frac{g_2'(\hat{x}, \hat{z})}{L_z} \, d\hat{z}$$

where q is the probability density, and g_2' and L_z are as defined in Eq. (15). ζ is generally referred to as the suspension ratio, and η may be called the net deposition ratio. These two dimensionless ratios are mutually complementary. Thus, if ζ is known, the net deposition ratio and, hence, the net deposition rate can be calculated from Eq. (24).

Utilizing the relations given in Appendix A and carrying out the integration indicated in Eq. (24), the expression for the suspension ratio can be obtained as follows:

For $\hat{V}_d \neq \hat{W}$ or $\hat{V}_2 \neq 0$,

$$\zeta(\hat{x}) = \frac{1}{2} \left[\operatorname{erfc}(\hat{W} \hat{x} - \hat{H}) - (\hat{V}_d / \hat{V}_2) \exp(4\hat{W} \hat{x} \hat{H}) \operatorname{erfc}(\hat{W} \hat{x} + \hat{H}) + (2\hat{V}_1 / \hat{V}_2) \exp\left\{4\hat{V}_d \hat{x} \hat{H} + 4 \hat{V}_d \hat{V}_2 \hat{x}^2\right\} \operatorname{erfc}(2\hat{V}_1 \hat{x} + \hat{H}) \right] \quad (25a)$$

This equation is indeterminate when $\hat{V}_d = \hat{W}$ or $\hat{V}_2 = 0$. For this case, $\zeta(\hat{x})$ can be determined by setting $\hat{W} = \hat{V}_d$ in the expression for g_2' in Eq. (15) and then integrating as indicated in Eq. (24). Alternately, one can take the limit of

Eq. (25a) as $\hat{W} \rightarrow \hat{V}_d$. The final expression for ζ in this case is as follows:

For $\hat{V}_d = \hat{W}$ or $\hat{V}_2 = 0$,

$$\begin{aligned} \zeta(\hat{x}) = & \frac{1}{2} \left[\operatorname{erfc}(\hat{V}_d \hat{x} - \hat{H}) \right. \\ & - (4\hat{V}_d \hat{x} / \sqrt{\pi}) \exp\left\{-\left(\hat{V}_d \hat{x} - \hat{H}\right)^2\right\} \\ & \left. + (1 + 4 \hat{V}_d \hat{x} \hat{H} + 4 \hat{V}_d^2 \hat{x}^2) \exp(4\hat{V}_d \hat{x} \hat{H}) \operatorname{erfc}(\hat{V}_d \hat{x} + \hat{H}) \right] \end{aligned} \quad (25b)$$

Equations (25a) and (25b) are consistent with the corresponding expressions for the net deposition rate given by Ermak (1977). These equations are applicable under all stability and mixing conditions. In the well-mixed region of the unstable and neutral cases, however, \hat{H} may be set to zero. For this case, $\zeta(\hat{x}) \equiv g_4'(\hat{x})$ and Eqs. (25a) and (25b) reduce to Eqs. (20d) and (20e), respectively.

The net deposition rate is a useful measure of pollutant deposition over a large area such as a pasture, farmland, or forest downwind of the source. The suspension ratio provides a check on mass conservation.

SECTION 4

RESULTS AND DISCUSSION

The algorithms developed in the previous section for various stability and mixing conditions for an elevated continuous point source were tested using the following numerical values for the model parameters:

$$U = 5 \text{ m/s} , V_d = W = 10 \text{ cm/s or } 0.$$

For stable conditions (P-G stability classes E and F, or KST = 5 and 6), the effective source height $H = 30$ m was used. For unstable/neutral conditions (P-G stability classes A, B, C, D, or KST = 1, 2, 3, 4), $H = 100$ m and $L = 1000$ m were used. For all stability conditions, values of $V_d > W$ were also used to test the algorithms. Some of the results, calculated up to a downwind distance of 20 km from the source, are presented and discussed in this section. These results include the variation with downwind distance of ground-level concentrations, vertical concentration profiles, surface deposition fluxes, and net deposition and suspension ratios.

The values of the dispersion parameters σ_y and σ_z used in the calculations are the P-G values (Pasquill, 1961; Gifford, 1960), which appear as graphs in

Turner (1970) and in Gifford (1976; Fig. 2). These values, which are used in the EPA models PAL (Petersen, 1978) and MPTER (Pierce and Turner, 1980), are most applicable to a surface roughness of 0.03 m (Pasquill, 1976).

GROUND-LEVEL CONCENTRATIONS (GLC)

The ground-level ($z = 0$) plume-centerline ($y = 0$) relative concentration, $C(x,0,0)/Q$, is shown in Figure 1 as a function of the downwind distance x for stable atmospheric conditions (class E). Three sets of deposition parameters were used: $V_d = W = 10, 5, 0$ cm/s. The last value, which refers to the limiting zero-deposition case in which the new deposition algorithms reduce to the existing Gaussian plume algorithms of EPA models, is included for comparison. The effect of deposition is seen as an increase in GLC near the source, and a compensating decrease farther downwind; the magnitude of the peak GLC increases, and it occurs closer to the source. This is a result of gravitational settling which tends to move the plume toward the ground as it travels downwind. The GLC curve for $V_d = W = 5$ cm/s, as expected, is in between the other two curves. In Fig. 1 (and several other figures in this section), the GLC are plotted as the abscissae and x as the ordinate. The arrangement, while differing from conventional practice, proved convenient for computer-plotting of results, using available software, to suit the report format.

Figure 2 shows the dependence of the new algorithms on the wind speed. For $V_d = W = 0$, $UC(x,0,0)/Q$ calculated from the well-known Gaussian plume algorithms is independent of the wind speed. For $V_d = W = 10$ cm/s, however, it is a func-

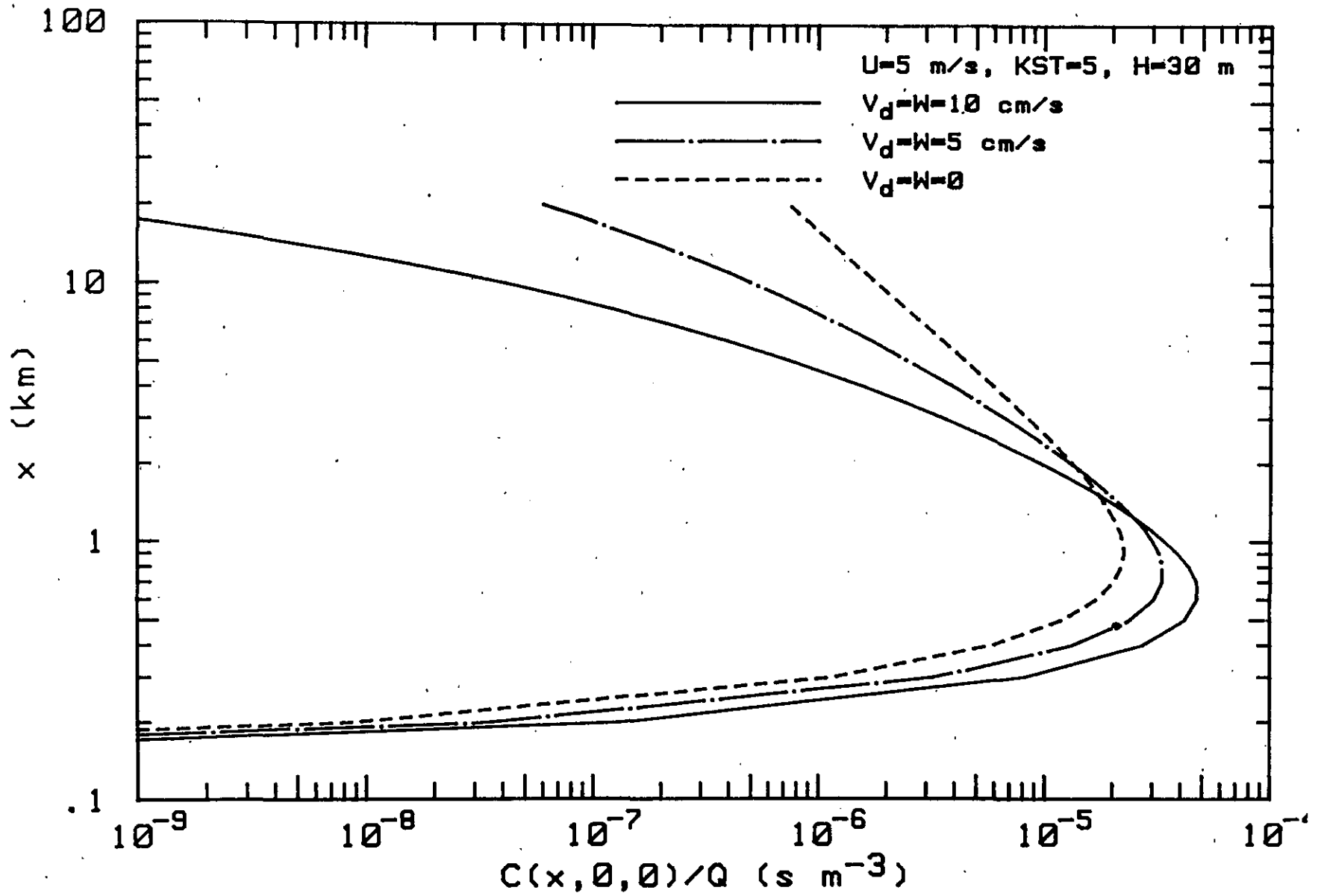


Figure 1. Variation of plume-centerline GLC with downwind distance for different values of $V_d = W$ under slightly stable conditions.

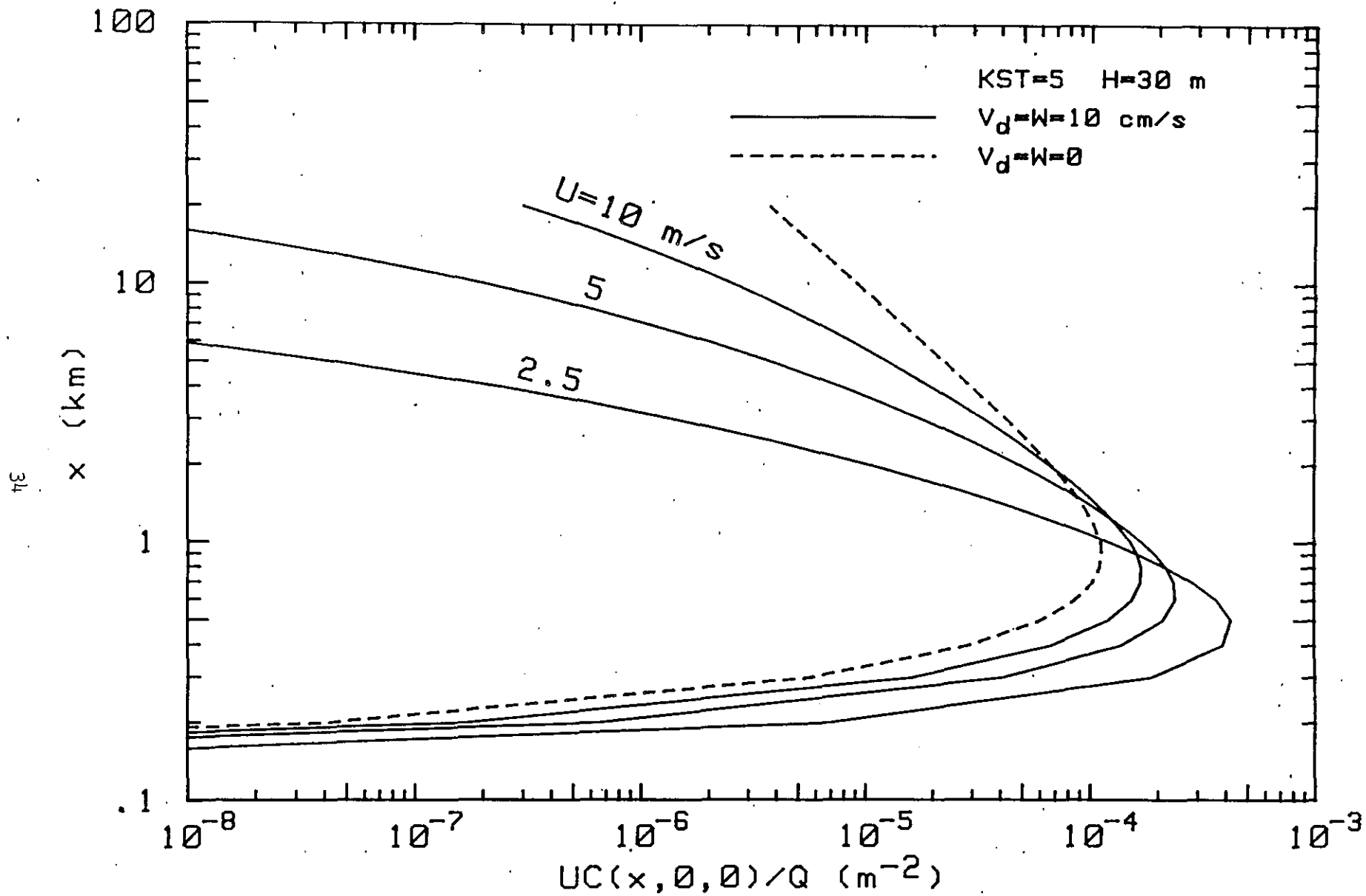


Figure 2. Variation of deposition effects on GLC for different values of wind speed.

tion of U , as shown in Fig. 2 for $U = 2.5, 5, 10$ m/s. In physical terms, more deposition takes place closer to the source at lower wind speeds. As U increases, the peak GLC moves farther away from the source. For a given set of $V_d = W > 0$ and increasingly large finite values of U , the values of $UC(x,0,0)/Q$ approach the curve for $V_d = W = 0$. This behavior can also be seen from Eq. (15). It should be noted that in the model test results presented in this section, some of the high wind speeds used are unlikely to occur in reality, at the source height indicated, with the chosen stability. They are included here primarily to illustrate the model behavior.

For unstable or neutral cases, concentrations are calculated by considering the multiple eddy reflections from the ground and the stable layer aloft; see Eq. (17). The GLC for P-G stability class C are shown in Figure 3 for $V_d = W = 10$ and 0 cm/s, and $V_d = 2$ and $W = 0.2$ cm/s. The last set of parameters are typical of small particles for which gravitational settling is insignificant. For this case, the deposition effects on the GLC are small and evident only far from the source. The reduction in the GLC is a direct result of ground deposition. In general, the effects of deposition are smaller than in the stable case (Fig. 1).

The GLC for P-G stability classes A to D are shown in Figure 4 for $V_d = W = 10$ and 0 cm/s. The effects of deposition on the GLC are the largest for class D, and decrease markedly as the atmosphere becomes more unstable; this is reasonable, since atmospheric turbulence enhances mixing of the plume, and distributes the material deficit at the surface through the plume's entire depth. For $L = 1000$ m, the criterion $\sigma_z(x) \geq 1.6 L$ for the well-mixed region

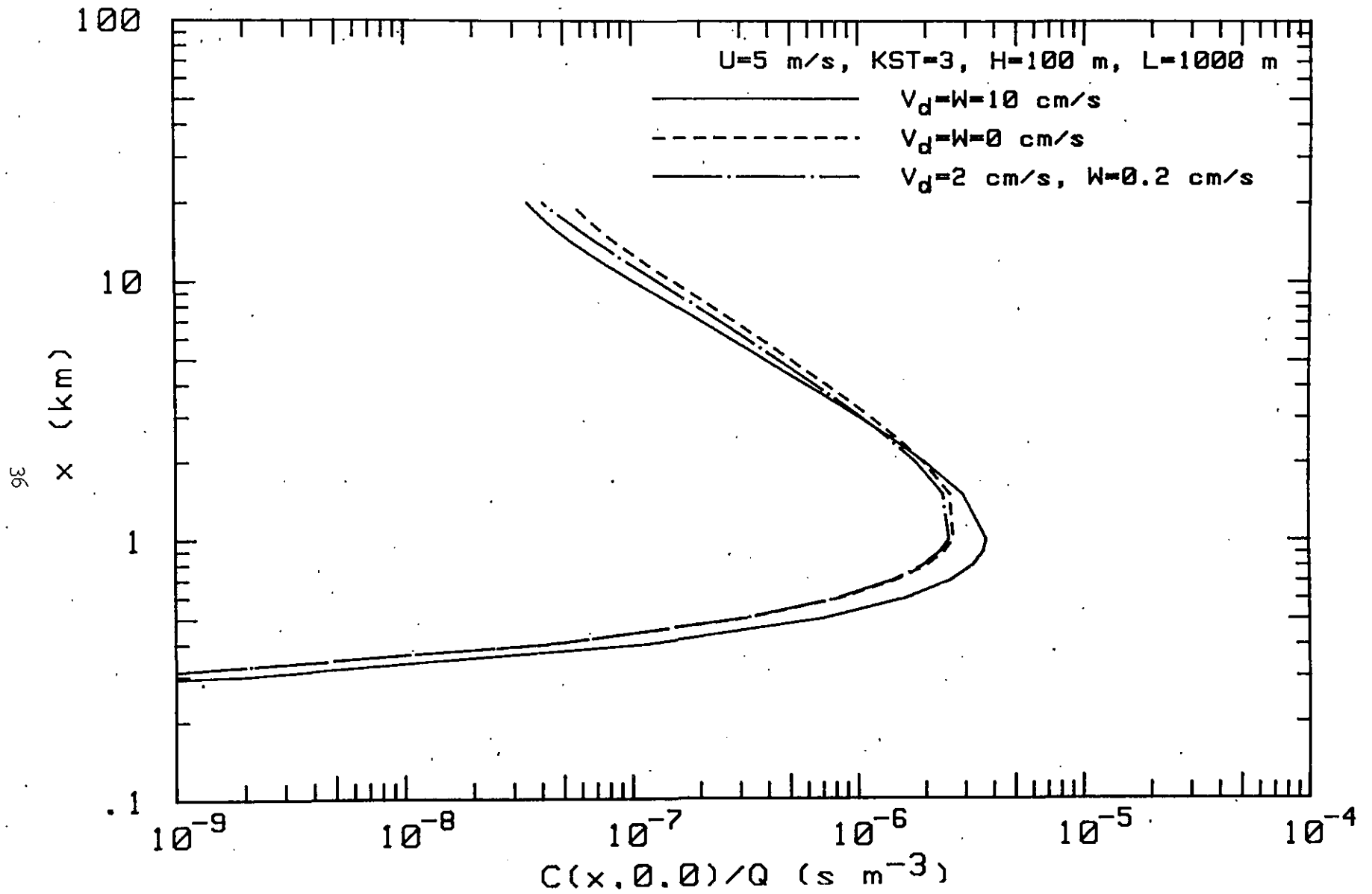


Figure 3. Variation of plume-centerline GLC with downwind distance for $V_d = W$ and $V_d > W$ under slightly unstable conditions.

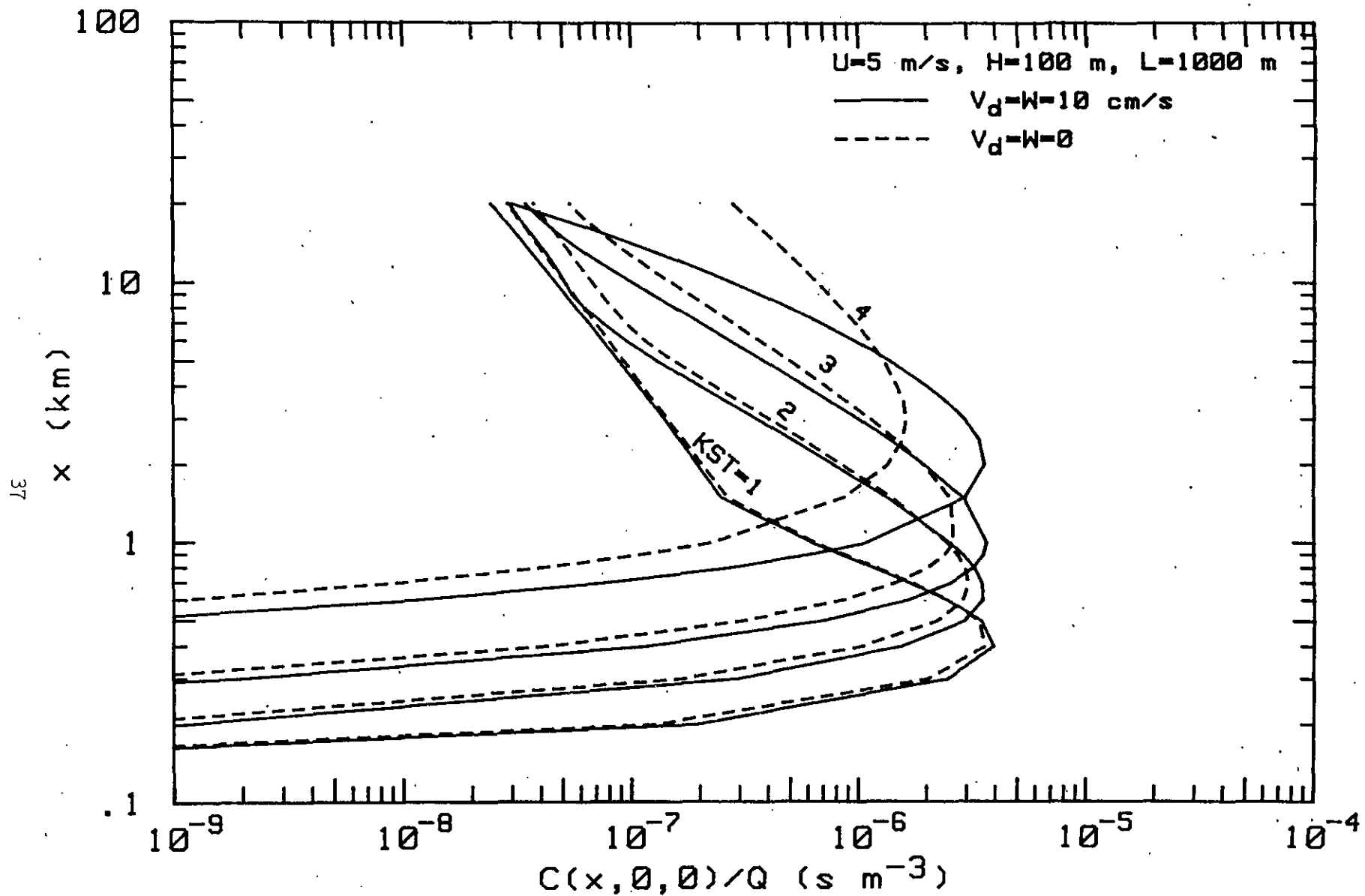


Figure 4. Variation of deposition effects on GLC for different unstable and neutral conditions.

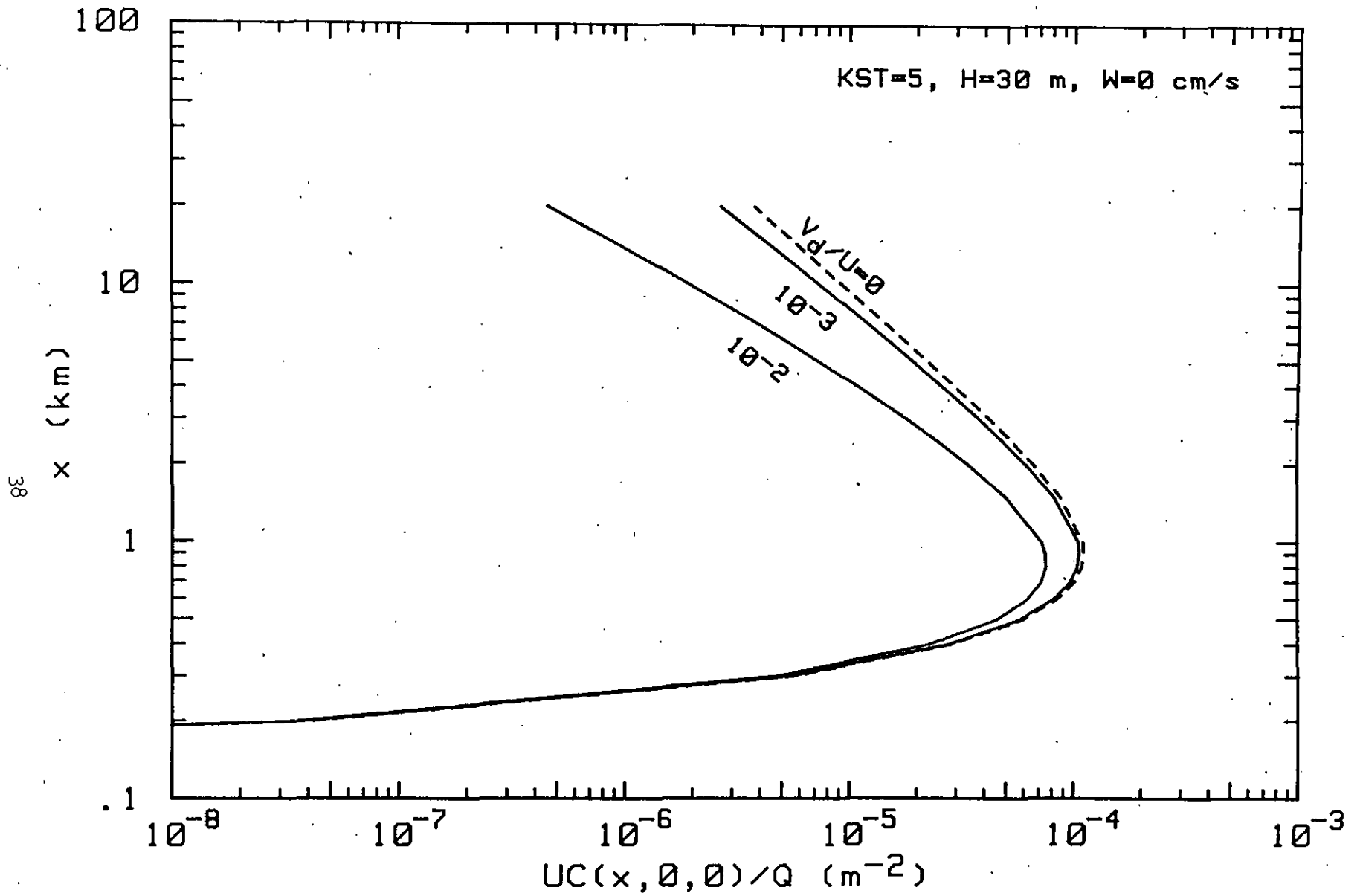


Figure 5. Variation of GLC of a gaseous pollutant ($W = 0$) for different values of the parameter V_d/U under slightly stable conditions.

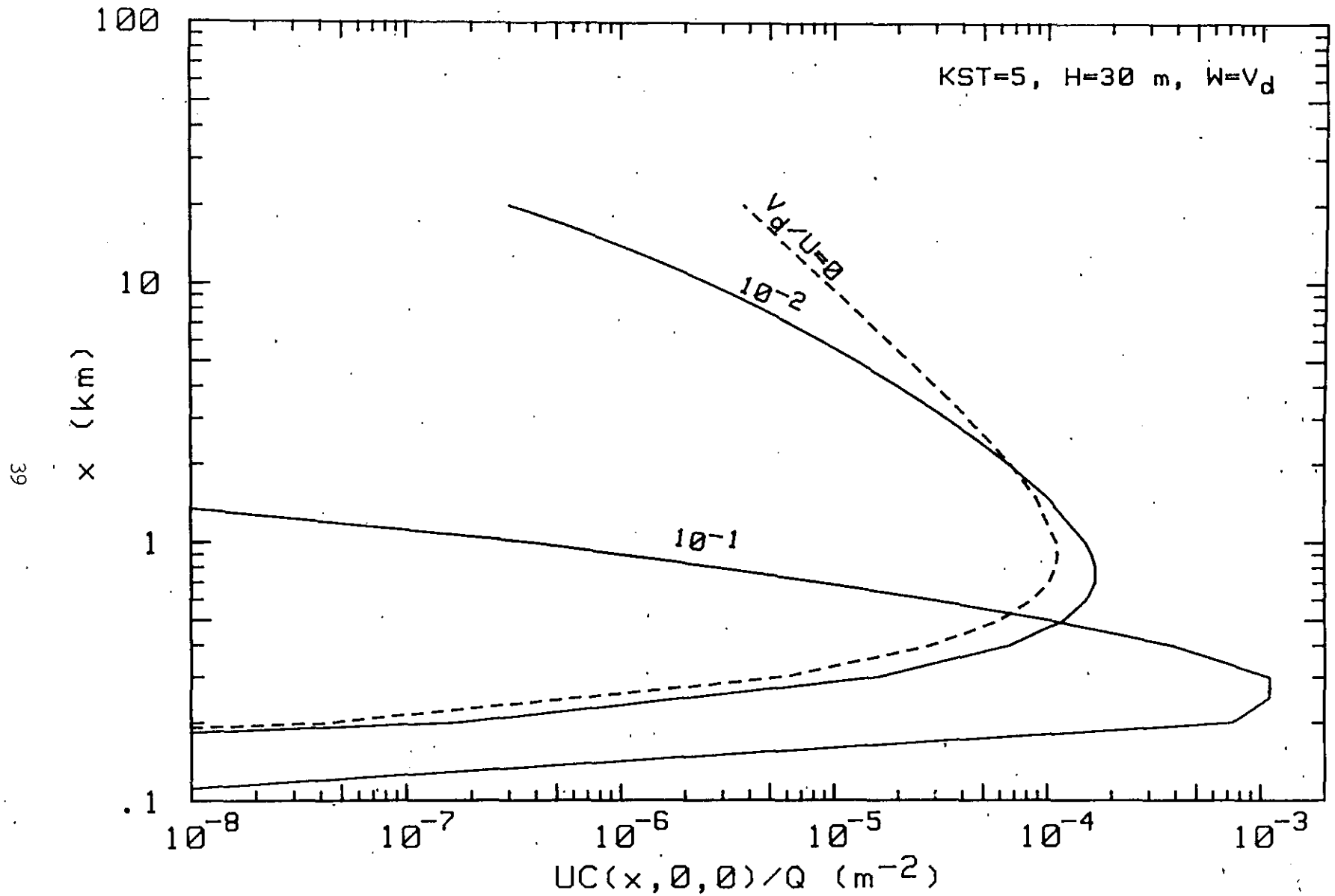


Figure 6. Variation of GLC of a particulate pollutant ($V_d = W$) for different values of the parameter V_d/U under slightly stable conditions.

is satisfied for $x \geq 1.81$ km and 11.54 km for stability classes A and B, respectively. For larger downwind distances, the plume gets thoroughly mixed, leading to a uniform concentration with height, given by Eq. (20), and the GLC decreases less rapidly with distance as shown in Fig. 4.

Figures 5 and 6 bring out the parameterization of the new algorithms for concentration in terms of $\hat{V}_d = V_d/U$ and $\hat{W} = W/U$. Figure 5 shows $UC(x,0,0)/Q$ versus x for $\hat{W} = 0$ and $\hat{V}_d = 10^{-2}$, 10^{-3} , and 0. These parameters are typical of the non-gravitational deposition of a gas. For $\hat{V}_d = 10^{-2}$, which represents the case of a moderately strong deposition, the GLC at $x = 20$ km for $KST = 5$ and $H = 30$ m is an order of magnitude smaller than the corresponding GLC for $\hat{V}_d = 0$. These results would remain the same, irrespective of the individual values of V_d and U provided \hat{V}_d remains constant. Deposition occurs entirely due to gravitational settling of the particles when $V_d = W > 0$ (see Appendix B). Figure 6 shows the corresponding results for particulate deposition for $\hat{V}_d = \hat{W} = 10^{-1}$, 10^{-2} , and 0. The first value refers to a case with strong gravitational settling; for example, $V_d = W = 10$ cm/s and $U = 1$ m/s. Note that the results shown in Fig. 2 correspond to $\hat{V}_d = \hat{W} = 10^{-2}$, 2×10^{-2} , and 4×10^{-2} .

CONCENTRATION PROFILES

For stable conditions (class E) and $\hat{V}_d = \hat{W} = 2 \times 10^{-2}$ and 0, particle concentration profiles are plotted in Figure 7 as $C(x,0,z)/Q$ versus z/H at three downwind locations. The effect of deposition is to tilt the plume towards the ground due to gravitational settling. At $x = 0.5$ km, this is seen to increase

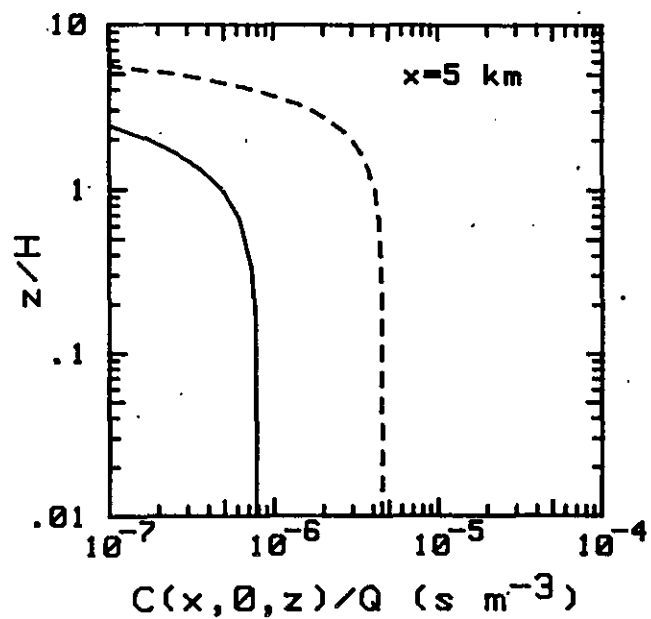
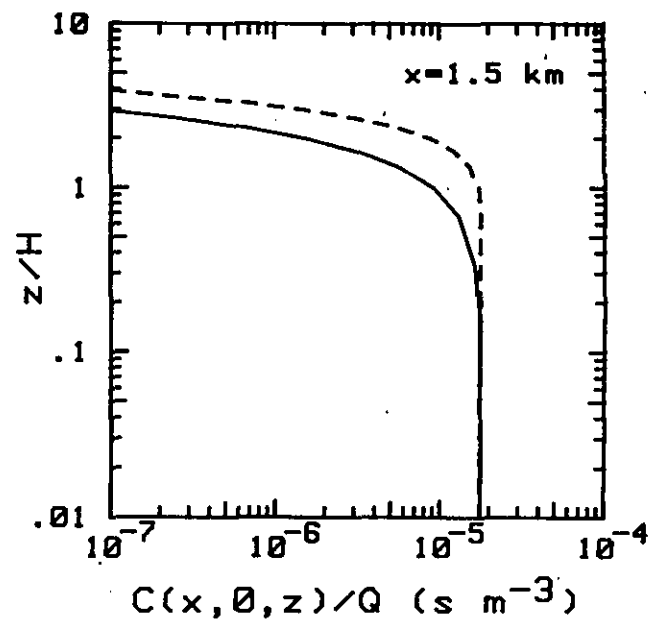
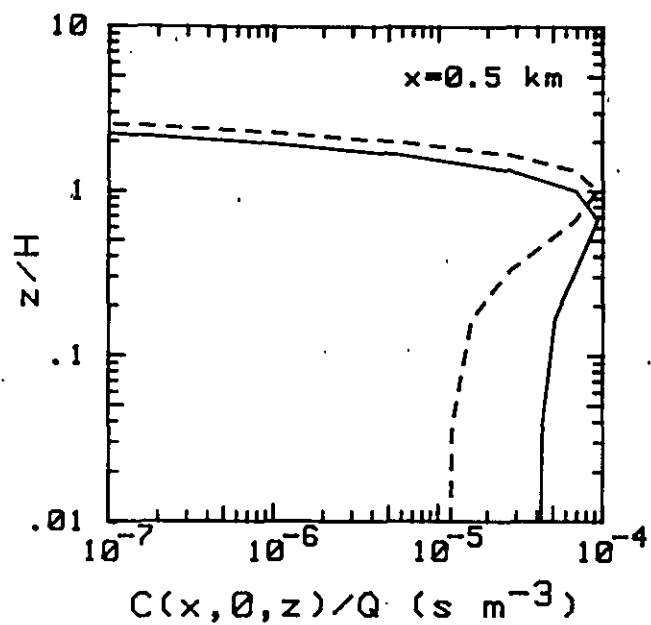


Figure 7. Deposition effects on vertical concentration profiles of a particulate pollutant under slightly stable conditions.

(KST = 5, H = 30 m, U = 5 m/s

— $V_d = W = 10 \text{ cm/s}$

- - - $V_d = W = 0$)

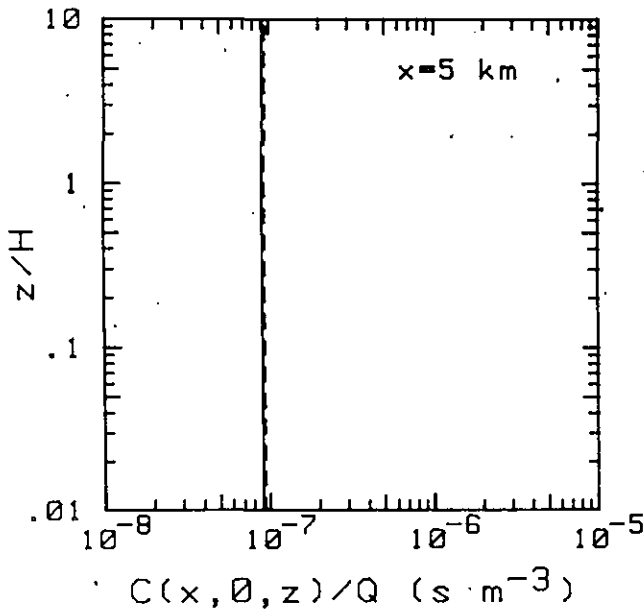
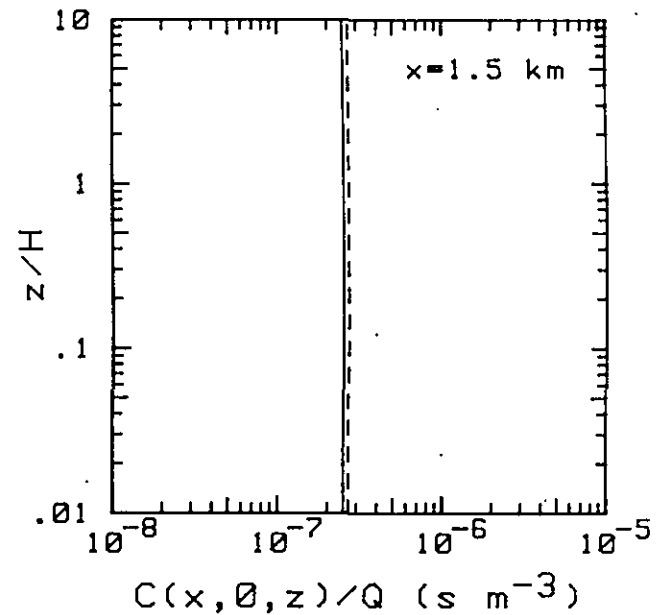
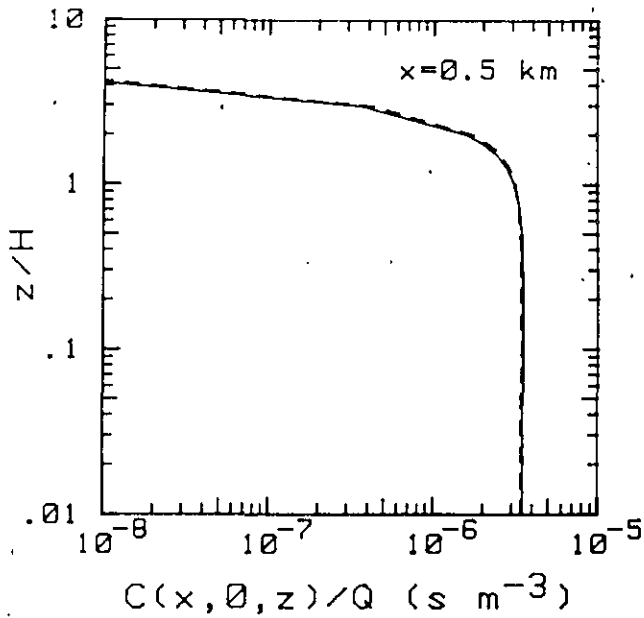


Figure 8. Deposition effects on vertical concentration profiles of a particulate pollutant under extremely unstable conditions.

(KST = 1, H = 100 m, U = 5 m/s,

L = 1000 m

— $V_d = W = 10 \text{ cm/s}$

- - - $V_d = W = 0$)

the concentration for $z/H < 1$, but decrease it at higher elevations. The magnitude of the peak elevated concentration increases and its height decreases. As x increases farther, the atmospheric concentrations near the surface start to decrease. At $x = 1.5$ km, the surface air concentrations are identical to the zero-deposition case. The reduction in concentration at the higher elevations is due to the loss of material to the ground by deposition. At $x = 5$ km, the concentrations at all elevations are much smaller than the case without deposition. The elevation of the upper edge of the plume is also substantially lower.

The corresponding plots for strongly unstable conditions (class A) are shown in Figure 8. It can be seen that the deposition effects on concentration are uniformly small at all elevations, and the concentration profiles are almost indistinguishable from the zero-deposition case. This is due to the large eddies and increased turbulent mixing in strongly convective cases that evenly distribute the ground-deposition loss through the entire depth of the plume. At $x = 1.5$ km, the concentration calculated from Eq. (17) is uniform with height due to the multiple eddy reflections from the ground and the stable layer at $z = L$. At $x = 5$ km, the plume is assumed to be thoroughly mixed, and concentration is calculated from Eq. (20).

COMPARISON WITH SOURCE DEPLETION MODEL

Figure 9 shows the comparison of GLC calculated from the analytical K-model and the source depletion model for slightly stable conditions ($KST = 5$), and $\hat{W} = 0$ and $\hat{V}_d = 4 \times 10^{-3}$. It can be seen that the source depletion model consis-

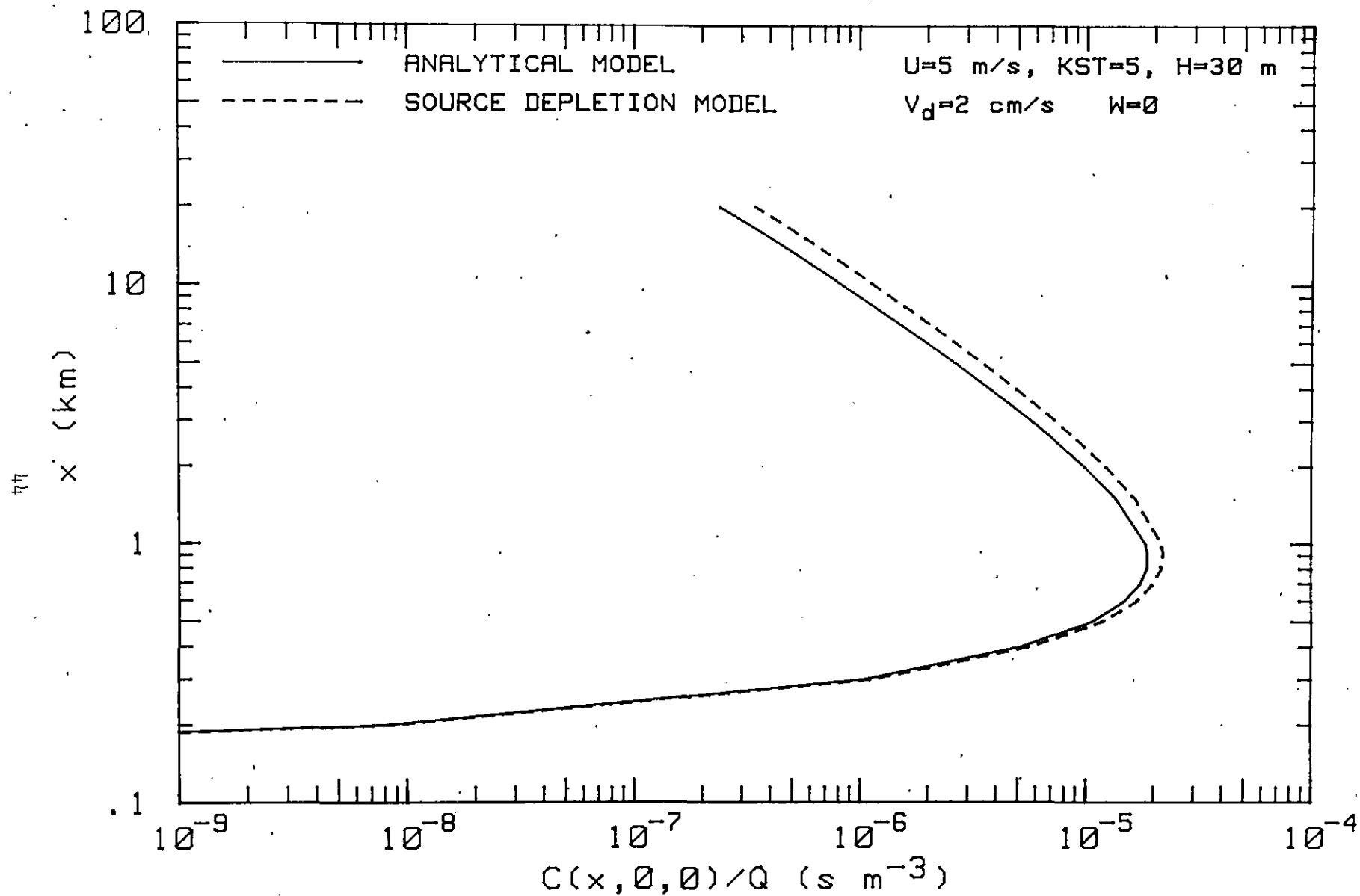


Figure 9. Variation of GLC of a gaseous pollutant under slightly stable conditions: comparison to classical source depletion model prediction.

tently overpredicts the GLC and, hence, the surface deposition flux; the GLC is about 50 percent higher in the source depletion model at $x = 20$ km. This difference is expected to increase with increasing deposition velocity and atmospheric stability. A source-depletion factor for the K-model can be derived from Eq. (16) as $(1 - 2 \sqrt{\pi} \hat{V}_d \hat{x} e^{\xi^2} \operatorname{erfc} \xi)$ where $\xi = \hat{H} + 2 \hat{V}_d \hat{x}$. The corresponding factor for the source depletion model (from Section 2), can be written as $\exp\{-\hat{V}_d \cdot I(\hat{x})\}$ where $I(\hat{x}) = \frac{2}{\sqrt{\pi}} \int_0^{\hat{x}} \exp(-\hat{H}^2) d\hat{x}'$. This is generally larger and, therefore, predicts larger relative concentrations.

Figure 10 shows the comparison of GLC calculated by the two models for the particulate deposition case of $\hat{V}_d = \hat{W} = 2 \times 10^{-2}$; other model parameters remain the same as before. It can be seen that the tilted-plume source depletion model (see Section 2) overpredicts the peak GLC by about 40 percent, though its downwind location is the same in both models. This overprediction near the source is compensated by an underprediction at large x . For any $\hat{V}_d \geq \hat{W} > 0$, the source-depletion factor for the K-model is given from Eq. (16) as $(1 - 2 \sqrt{\pi} \hat{V}_1 \hat{x} e^{\xi^2} \operatorname{erfc} \xi)$, where $\xi = \hat{H} + 2 \hat{V}_1 \hat{x}$, and $\hat{V}_1 = \hat{V}_d - \hat{W}/2$. The corresponding factor for the tilted-plume source depletion model can be written as $\exp\{-\hat{V}_d \cdot I(\hat{x})\}$, where $I(\hat{x}) = \frac{2}{\sqrt{\pi}} \int_0^{\hat{x}} \exp\{-(\hat{H} - \hat{W} \hat{x}')^2\} d\hat{x}'$. This suggests that the straightforward analytical algorithms of the K-theory model are preferable to the evaluation of the integral $I(\hat{x})$, with a sharply-peaked skewed integrand, for each x , H , W/U , and stability class.

For a ground-level source ($H = 0$) and $\hat{V}_d > \hat{W} = 0$, the vertical gaseous concentration profile in the source depletion model is given by

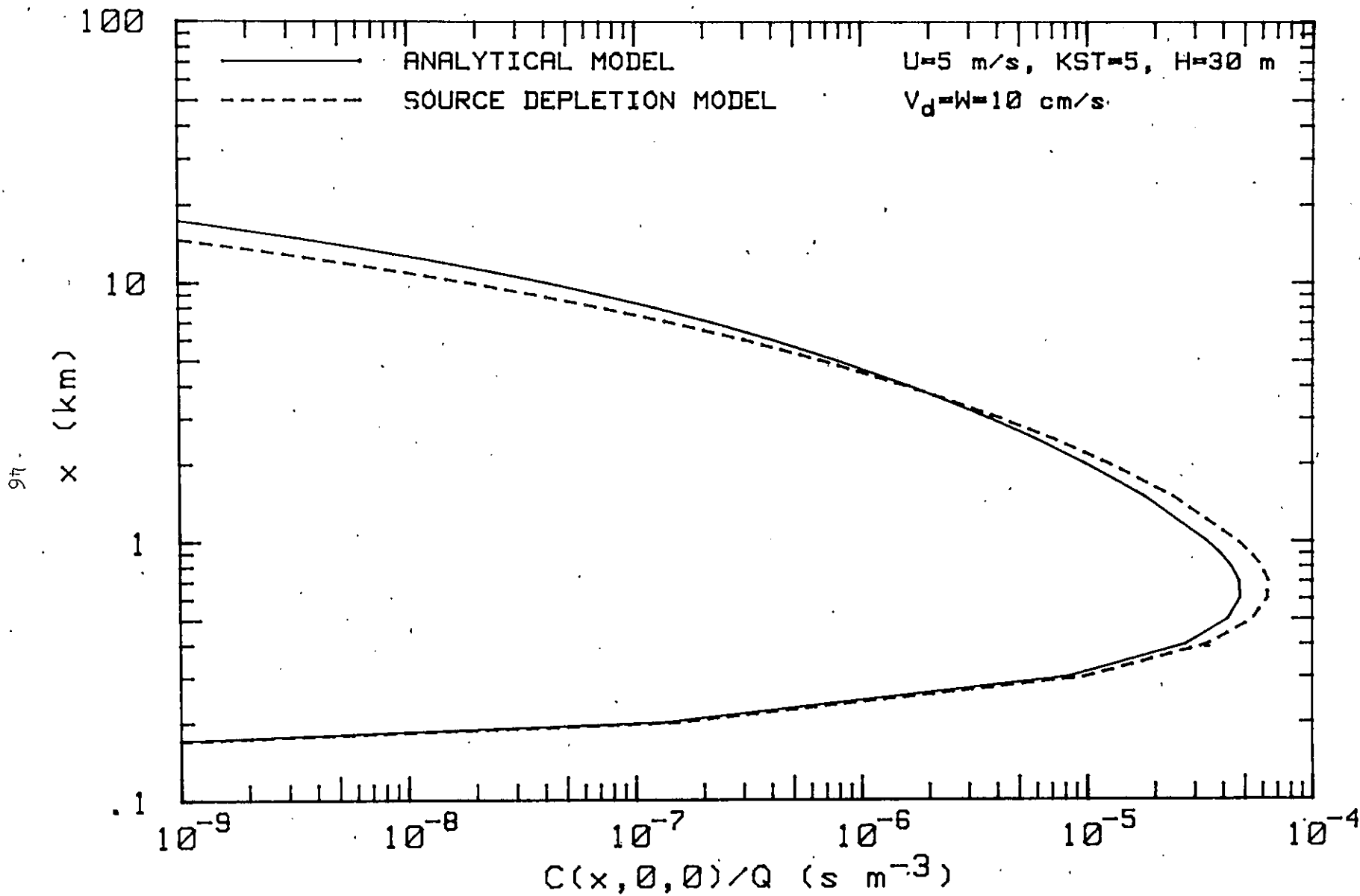


Figure 10. Variation of GLC of a particulate pollutant under slightly stable conditions: comparison to tilted-plume source depletion model prediction.

$$\frac{C(\hat{x}, 0, \hat{z})}{Q} = \frac{1}{\pi \sigma_y \sigma_z U} \exp(-\hat{z}^2) \cdot \exp\{ -\hat{V}_d \cdot I(\hat{x}) \} ,$$

where $I(\hat{x}) = \frac{2}{\sqrt{\pi}} \int_0^{\hat{x}} d\hat{x}'$. This equation predicts that the maximum concentration occurs at the ground level at all x . This is not the case for the K-theory model, since the removal of material through the depth of the plume depends on the intensity of vertical mixing. Here the vertical concentration profile is given by

$$\frac{C(\hat{x}, 0, \hat{z})}{Q} = \frac{1}{\pi \sigma_y \sigma_z U} \exp(-\hat{z}^2) \cdot (1 - 2 \sqrt{\pi} \hat{V}_d \hat{x} e^{\xi^2} \operatorname{erfc} \xi),$$

where $\xi = \hat{z} + 2 \hat{V}_d \hat{x}$. The shape of this concentration profile changes with x . A rapid depletion at the bottom portion of the plume occurs, and the concentration gradient with height then becomes slightly positive near the ground. Downwind of the source, the height of the maximum concentration is above the ground and increases with x . This height is independent of the deposition velocity at large distances downwind from the source.

SURFACE DEPOSITION FLUXES

The surface flux, $D(x,y)$, is calculated directly from Equation (22). The relative surface deposition flux along plume centerline, $D(x,0)/Q$, is plotted against the downwind distance in Figure 11 for stable conditions (classes E and F). The model parameters used are $H = 30$ m, $\hat{V}_d = \hat{W} = 2 \times 10^{-2}$. The downwind variation of the particle surface deposition flux is identical to the correspond-

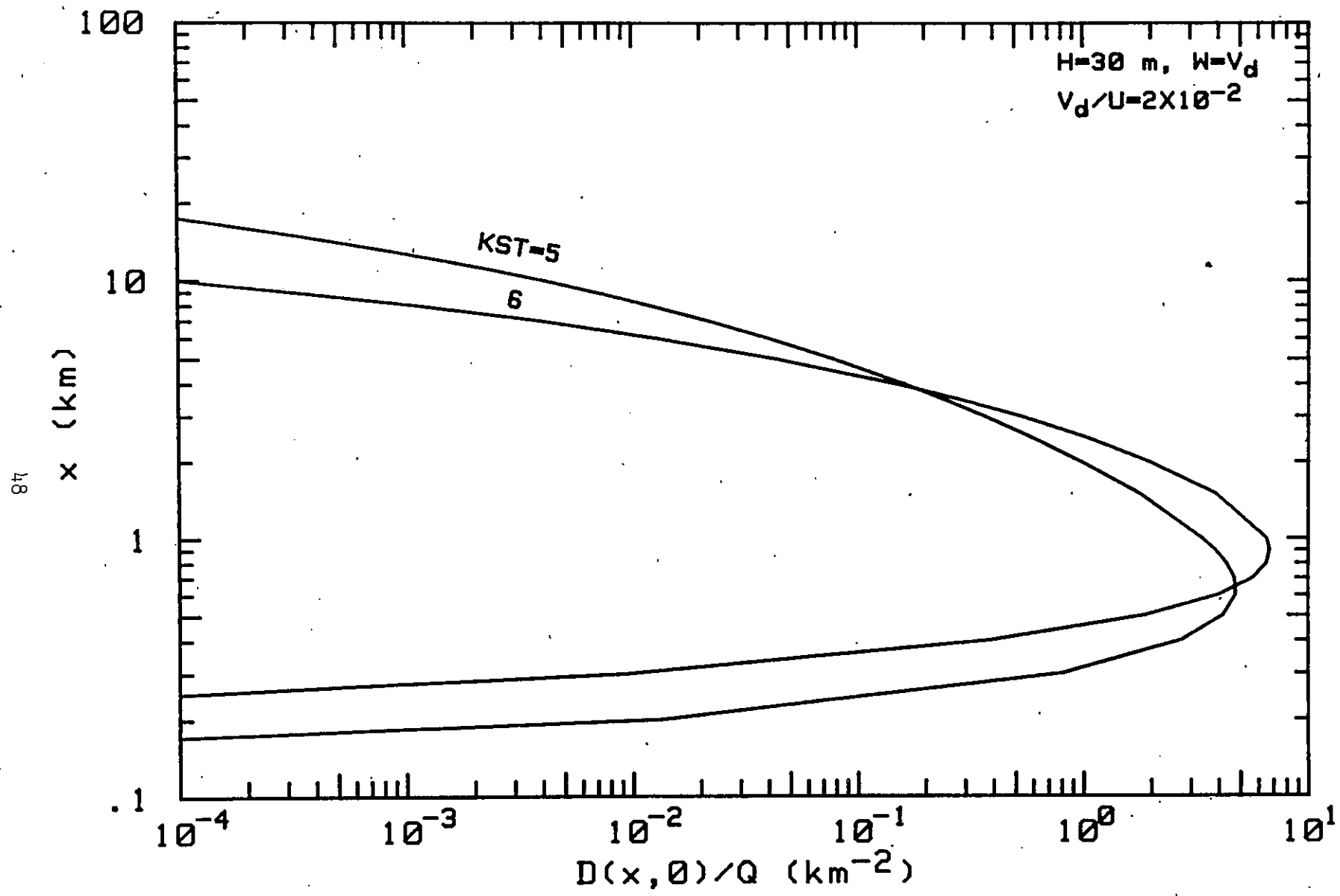


Figure 11. Variation of surface deposition flux of particles with downwind distance under stable conditions.

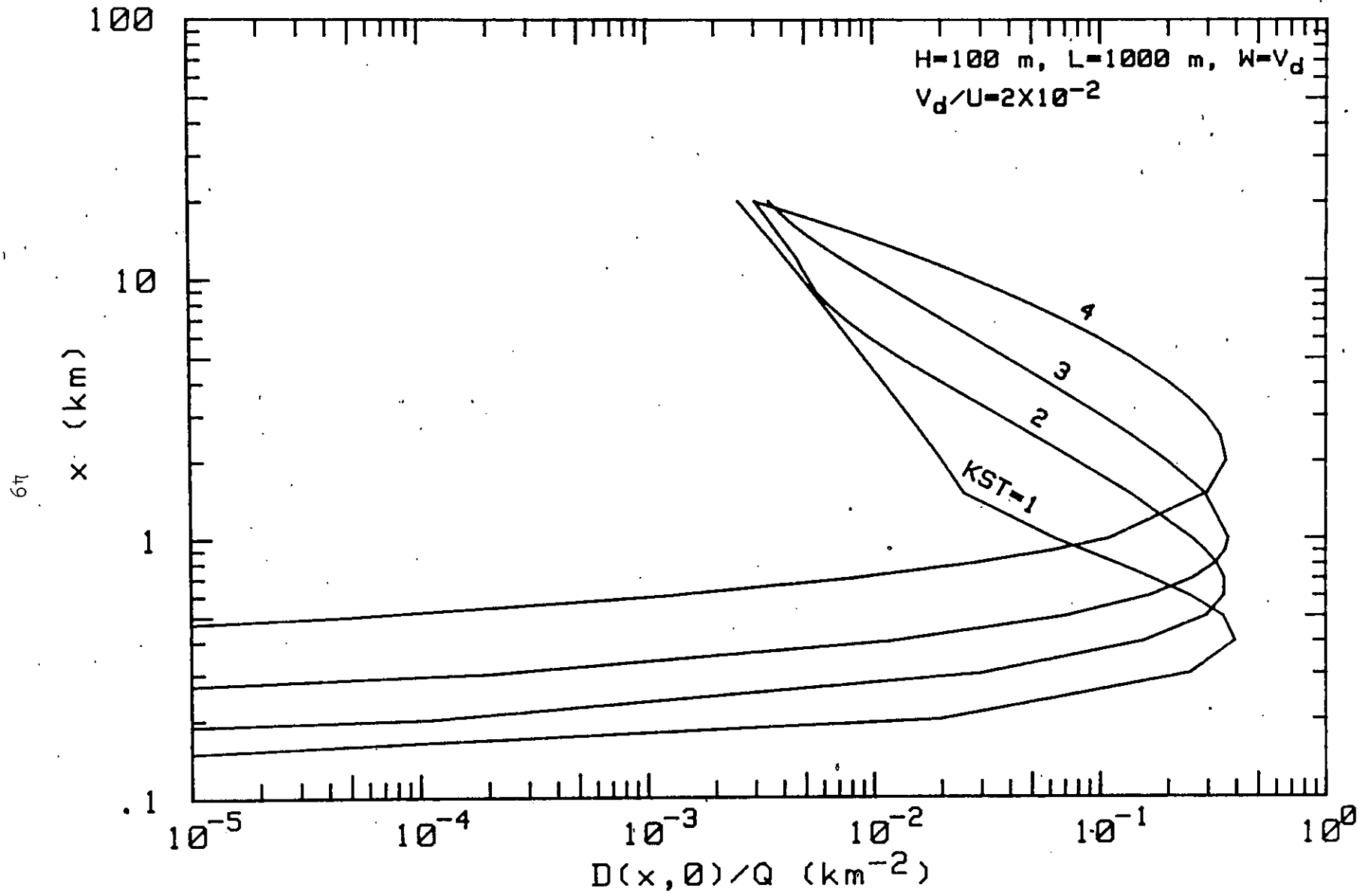


Figure 12. Variation of surface deposition flux of particles with downwind distance under unstable and neutral conditions.

ing variation of the GLC discussed earlier. As the value of $\hat{V}_d = \hat{W}$ is increased, the peak value of $D(x,0)$ increases and occurs closer to the source due to the gravitational settling of the plume. This, however, will not be the case for $\hat{W} = 0$ where, for large values of $\hat{V}_d \hat{x}$, there will be only a negligible increase in surface deposition flux due to increases in the deposition velocity (Ermak, 1977).

The surface deposition flux results for stability classes A to D are shown in Figure 12. The model parameters used are $H = 100$ m, $L = 1000$ m, and $\hat{V}_d = \hat{W} = 2 \times 10^{-2}$. It can be seen that the downwind variation of $D(x,0)$ is analogous to the corresponding GLC variation shown in Fig. 4.

NET DEPOSITION AND SUSPENSION RATIOS

The net deposition and suspension ratios, calculated from Equations (24) and (25), are shown in Figures 13 and 14 for the stable and unstable/neutral conditions, respectively. The model parameters used are the same as given above. In general, as the stability increases, the entire particle deposition occurs closer to the source. For example, for stability class E, the total amount of pollutant released is deposited over a downwind distance of 12 km; for class F, the corresponding distance is only 7 km. For stability classes A to D, the net deposition within 20 km from the source is 12, 20, 47, and 95 percent, respectively, of the total amount released; the remainder is still suspended in the air to be deposited farther downwind. Thus, for a given set of \hat{W} and $\hat{V}_d \neq 0$, the pollutant travel distance increases significantly due to the increased turbulence of

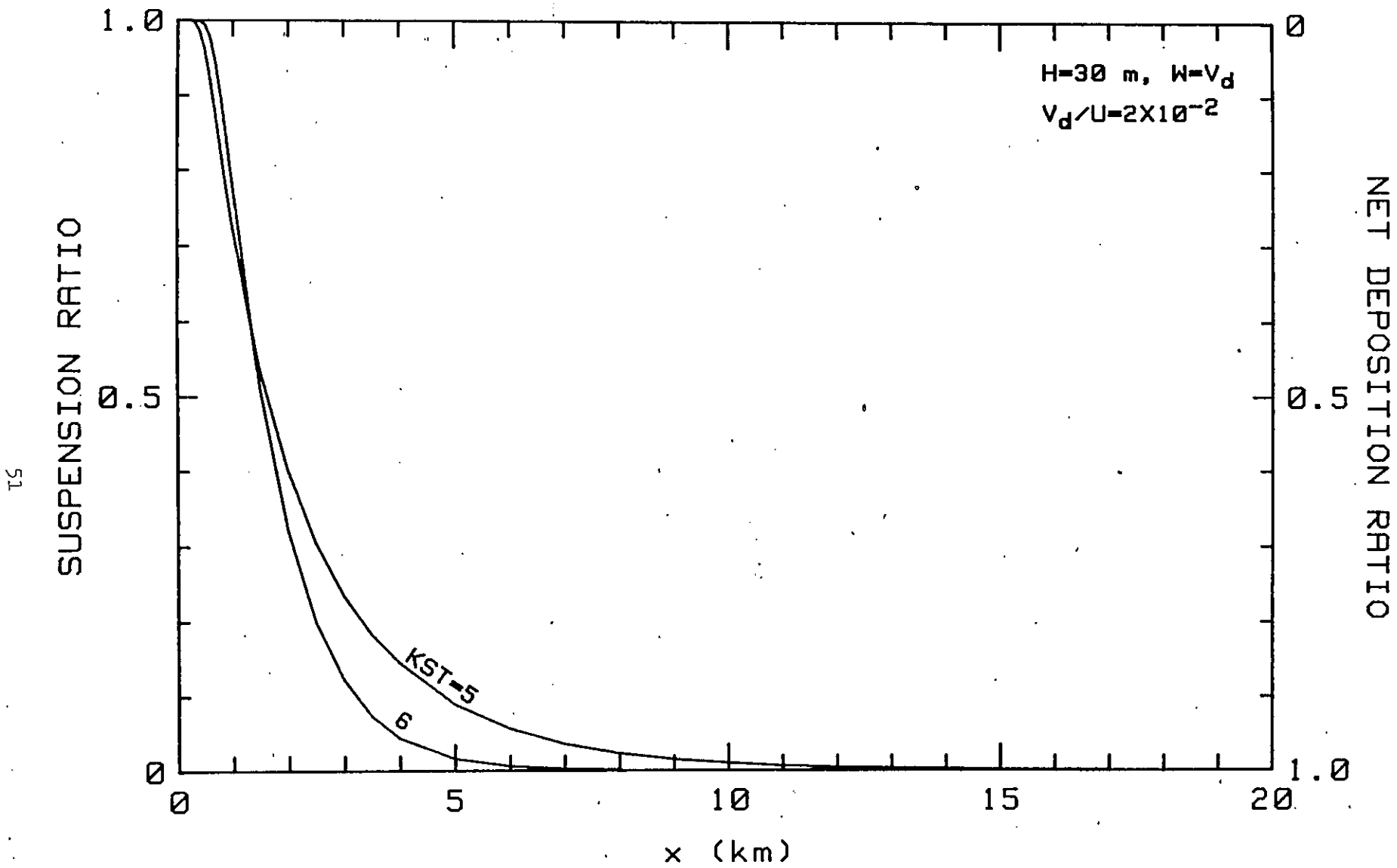


Figure 13. Variation of net deposition and suspension ratios of particulate pollutant with downwind distance under stable conditions.

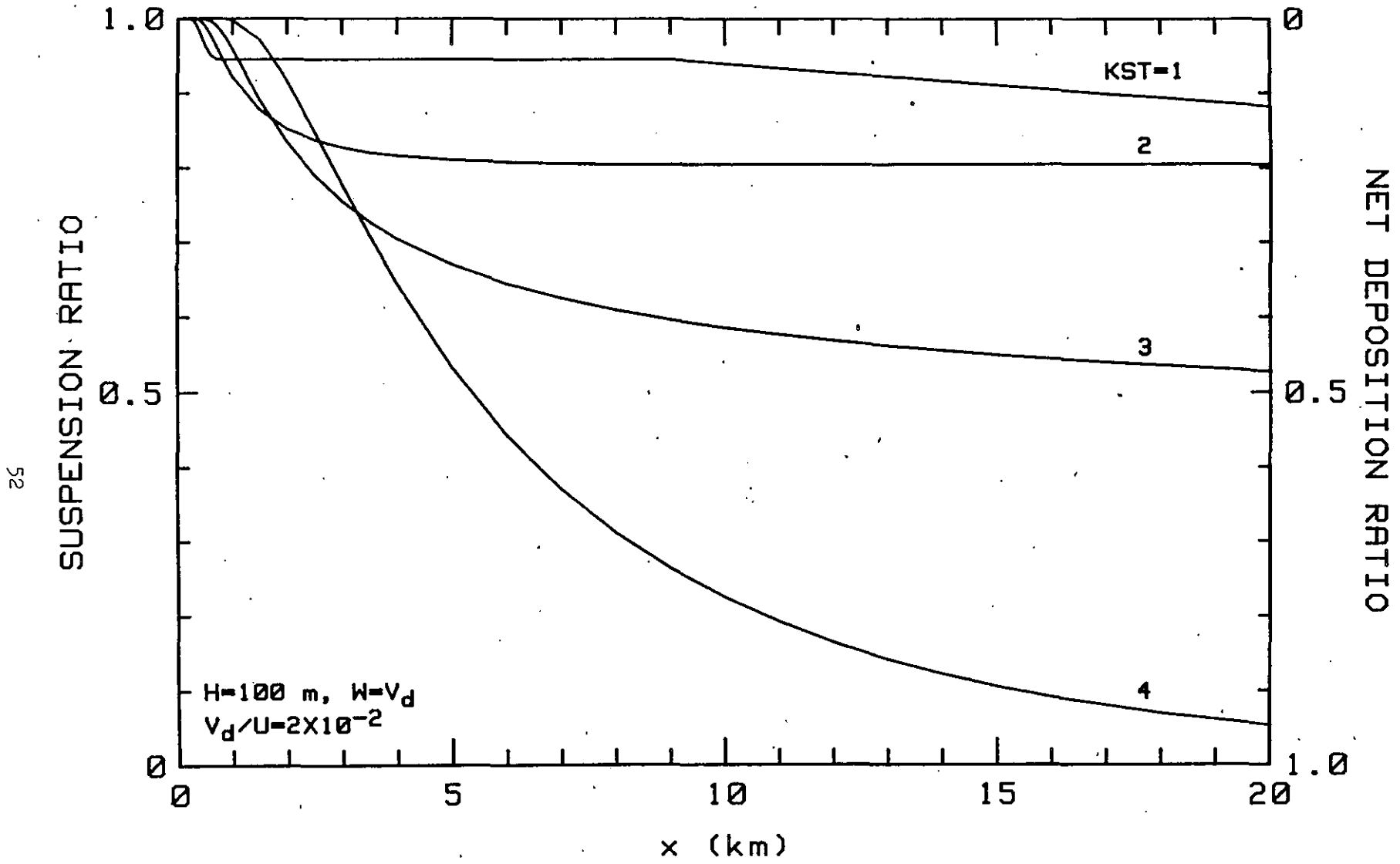


Figure 14. Variation of net deposition and suspension ratios of particulate pollutant with downwind distance under unstable and neutral conditions.

the atmosphere which disperses the pollutants over a much wider area.

In general, as the deposition velocity is increased, ground deposition occurs closer to the source. Therefore, a smaller surface area is contaminated but at a higher flux value. For a given \hat{H} and comparable values of $\hat{V}_1 \hat{x}$, there is a significant difference between the two classes $\hat{V}_d > \hat{W} = 0$ and $\hat{V}_d = \hat{W} > 0$ in the rate at which the final 10 - 20% of pollutant is deposited on the ground (Ermak, 1977). The rate is much faster for particles where $\hat{W} = \hat{V}_d$, since the gravitational settling tends to transport the particles at a constant rate toward the ground where they are removed. For gases, where $\hat{W} = 0$, only the atmospheric diffusion acts to bring the pollutant into contact with the ground. The random nature of turbulent diffusion process makes it a much slower removal process than gravitational settling for transport over long distances.

SECTION 5

CONCLUSIONS

An atmospheric transport and deposition model has been formulated for gaseous or suspended particulate pollutants emitted from an elevated point source. This analytical model, based on the gradient-transfer or K-theory, treats gravitational settling and dry deposition in a more physically realistic and straightforward manner than the usual tilted-plume source depletion approach. For practical application of the model to a variety of atmospheric stability conditions, the eddy diffusivity coefficients in the analytical solutions have been expressed in terms of the widely-used Gaussian plume dispersion parameters, which are functions of downwind distance and stability class. This allows one to utilize the vast amount of empirical data on these parameters, for a variety of diffusion conditions, within the framework of the standard turbulence-typing schemes.

In order to facilitate comparison, the new diffusion-deposition algorithms for various stability and mixing conditions have been presented as analytical extensions of the well-known Gaussian plume diffusion algorithms presently used in EPA models. In the limit when settling and deposition velocities are zero, the new algorithms reduce to the current Gaussian plume equations. Thus the atmospheric transport and deposition model outlined here retains the ease

of application, and is subject to the same basic assumptions and limitations, associated with Gaussian plume-type models.

The parameterized deposition model has been applied to study two important deposition cases: (1) pollutant particles with appreciable settling velocity equal to the dry deposition velocity, and (2) gases or fine suspended particles which deposit on the ground without significant settling. The variation with downwind distance of ground-level concentrations, vertical concentration profiles, surface deposition fluxes, and net deposition and suspension ratios are presented. The values of the deposition velocity and the atmospheric stability are shown to have significant effects on these results.

Four types of Gaussian diffusion-deposition models have been briefly reviewed, and the ground-level concentrations of the present analytical gradient-transfer model have been compared with the corresponding results of the source depletion model. A systematic comparison of the performance of the various models has not been done so far, and none of them has been satisfactorily tested against observations. General statements on the relative merits and deficiencies of the various models in the literature are, at present, somewhat subjective, and largely rely on the key physical assumptions used in the model formulations and the complexity of the methods.

A field study has been proposed in Appendix C to measure one or more of the model parameters, and to obtain a good data set for model validation over a distance of at least 10 km from the source. The proposed study, based on a modified Bowen ratio-turbulent variance approach that avoids the difficulties associated

with the well-known vertical gradient and eddy-correlation methods, will provide needed data on mean concentrations, ground deposition flux, and deposition velocity.

REFERENCES

- Baron, T., E. R. Gerhard and H. F. Johnstone, 1949: Dissemination of aerosol particles dispersed from stacks. Ind. Chem.Eng. 41, 2403-2408.
- Berkowicz, R., and L. P. Prahm, 1978: Pseudospectral simulation of dry deposition from a point source. Atmospheric Environment 12, 379-389.
- Calder, K. L., 1961: Atmospheric diffusion of particulate material considered as a boundary value problem. J. Meteorol. 18, 413-416.
- Carslaw, H. S., and J. C. Jaeger, 1959: Conduction of Heat in Solids, 2nd ed. Oxford University Press, London.
- Chamberlain, A. C., 1953: Aspects of travel and deposition of aerosol and vapor clouds. A.E.R.E. Report H.P.-1261, Atomic Energy Research Estab., Harwell, Berks., U.K., 32 pp.
- Csanady, G. T., 1955: Dispersal of dust particles from elevated sources. Australian J. Phys. 8, 545-550.
- _____, 1957: Dispersal of dust particles from elevated sources. II. Limitations of the approximate theory. Australian J. Phys. 10, 558-564.
- _____, 1958: Deposition of dust particles from industrial stacks. Australian J. Appli. Sci. 9, 1-8.
- Ermak, D. L., 1977: An analytical model for air pollutant transport and deposition from a point source. Atmospheric Environment 11, 231-237.
- Fisher, B. E. A., 1979: Use of the diffusion approximation to model atmospheric dispersion over short and long distances. Mathematical Modeling of Turbulent Diffusion in the Environment. C. J. Harris, ed., Academic Press, New York, 237-275.
- Gifford, F. A., 1960: Atmospheric dispersion calculations using the generalized Gaussian plume model. Nuclear Safety 2, 56-59.
- _____, 1968: An outline of theories of diffusion in the lower layers of the atmosphere. Chapter 3, Meteorology and Atomic Energy 1968, D. H. Slade, ed.; available as TID-24190, NTIS, Springfield, VA, 65-116.
- _____, 1976: Turbulent diffusion-typing schemes: A review. Nuclear Safety 17, 68-86.

- Hanna, S. R., G. A. Briggs, J. Deardorff, B. A. Egan, F. A. Gifford and F. Pasquill, 1977: AMS workshop on stability classification schemes and sigma curves - summary of recommendations. Bull. Amer. Meteorol. Soc. 58, 1305-1309.
- Heines, T. S., and L. K. Peters, 1974: The effect of ground level absorption on the dispersion of pollutants in the atmosphere. Atmospheric Environment 8, 1143-1153.
- Horst, T. W., 1974: A surface depletion model for deposition from a Gaussian plume. Atmosphere-Surface Exchange of Particulate and Gaseous Pollutants (1974), available as CONF-740921, NTIS, Springfield, VA, 423-433.
- _____, 1976: The estimation of air concentrations due to the suspension of surface contamination by the wind. BNWL-2047, Battelle Pacific Northwest Labs., Richland, WA, 41pp.
- _____, 1977: A surface depletion model for deposition from a Gaussian plume. Atmospheric Environment, 11, 41-46.
- _____, 1979: A review of Gaussian diffusion-deposition models. Atmospheric Sulfur Deposition: Environmental Impact and Health Effects. D. S. Shriner, C. R. Richmond, and S. E. Lindberg, eds., Ann Arbor Science, Ann Arbor, MI, 1980.
- Hosker, R. P., 1980: Practical application of air pollutant deposition models -- current status, data requirements, and research needs. Proc. Internat. Conf. on Air Pollutants and Their Effects on the Terrestrial Ecosystem, S. V. Krupa and A. H. Legge, eds., John Wiley and Sons, New York. ATDL Contribution 80/8, NOAA, Oak Ridge, TN., 71pp.
- Izrael, Y. A., J. E. Mikhailova and A. J. Pressman, 1979: A model for operative evaluation of transboundary flows of pollutants. WMO Symposium on the Long-Range Transport of Pollutants and its Relation to General Circulation Including Stratospheric/Tropospheric Exchange Processes. WMO No. 538, Geneva, Switzerland, 271-279.
- Monin, A. S., 1959: On the boundary condition on the earth surface for diffusing pollution. Adv. Geophys. 6, 435-436.
- Overcamp, T. J., 1976: A general Gaussian diffusion-deposition model for elevated point sources. J. Appl. Meteorol. 15, 1167-1171.
- Pasquill, F., 1961: The estimation of the dispersion of windborne material. Meteorol. Mag. 90, 33-49.
- _____, 1976: Atmospheric dispersion parameters in Gaussian plume modeling. Part II. Possible requirements for change in the Turner Workbook values. EPA-600/4-76-030b. U.S. E.P.A., Research Triangle Park, N.C., 44pp.

- Petersen, W. B., 1978: User's Guide for PAL: A Gaussian-plume algorithm for point, area, and line sources. EPA-600/4-78-013. U.S. E.P.A., Research Triangle Park, N.C., 247pp.
- Pierce, T. E., and D. B. Turner, 1980: Users's Guide for MPTER: A multiple point Gaussian dispersion algorithm with optional terrain adjustment. EPA-600/8-80-016. U.S. E.P.A., Research Triangle Park, N.C., 247pp.
- Prahn, L. P., and R. Berkowicz, 1978: Predicting concentrations in plumes subject to dry deposition. Nature 271, 232-234.
- Rao, K. S., 1975: Models for sulfur oxide dispersion from the Northport power station. The LILCO/Town of Huntington Sulfates Program, Project Report P-1336, Environmental Research & Technology, Inc., Concord, MA.
- _____, and L. Satterfield, 1980: A study of the probable environmental impact of fugitive coal dust emissions at the Ravenswood Power Plant, New York. ATDL contribution 80/26, NOAA, Oak Ridge, TN, 86pp.
- Rounds, W., 1955: Solutions of the two-dimensional diffusion equations. Trans. Amer. Geophys. Union 36, 395-405.
- Scriven, R. A., and B. E. A. Fisher, 1975: The long range transport of airborne material and its removal by deposition and washout-II. The effect of turbulent diffusion. Atmospheric Environment 9, 59-68.
- Smith, F. B., 1962: The problem of deposition in atmospheric diffusion of particulate matter. J. Atmos. Sci. 19, 429-434.
- Turner, D. B., 1970: Workbook of Atmospheric Dispersion Estimates. Public Health Service Publication No. 999-AP-26, U.S. E.P.A., Research Triangle Park, N.C., 84pp.
- Van der Hoven, I., 1968: Deposition of particles and gases. Section 5-3, Meteorology and Atomic Energy 1968, D. H. Slade, ed.; available as TID-24190, NTIS, Springfield, VA, 202-208.
- Yamartino, R. J., 1981: Solutions to the equation for surface depletion of a Gaussian plume. 12th NATO/CCMS Internat. Tech. Meeting on Air Pollution Modeling and its Application, Palo Alto, Calif., 14 pp.

APPENDIX A

PROPERTIES OF ERROR FUNCTION AND OTHER RELATIONS

The error function is defined as

$$\operatorname{erf}(z) = \frac{2}{\sqrt{\pi}} \int_0^z e^{-t^2} dt \quad (\text{A-1})$$

The complementary error function is defined as

$$\operatorname{erfc}(z) = \frac{2}{\sqrt{\pi}} \int_z^{\infty} e^{-t^2} dt \quad (\text{A-2})$$

The normal probability integral function is defined as

$$\phi(z) = \frac{1}{\sqrt{2\pi}} \int_{-\infty}^z e^{-t^2/2} dt \quad (\text{A-3})$$

Eq. (A-3) gives the area under the normal probability curve. The three functions given above are related as follows:

$$\operatorname{erfc}(z) = 1 - \operatorname{erf}(z) \quad (\text{A-4})$$

$$\operatorname{erfc}(z) = 2[1 - \phi(\sqrt{2} z)] \quad (\text{A-5})$$

$$\operatorname{erf}(z) = 2 \phi(\sqrt{2} z) - 1 \quad (\text{A-6})$$

The symmetry relations are

$$\operatorname{erf}(-z) = -\operatorname{erf}(z) \quad (\text{A-7})$$

$$\operatorname{erfc}(-z) = 2 - \operatorname{erfc}(z) \quad (\text{A-8})$$

The values at the limits are

$$\operatorname{erf}(0) = 0, \quad \operatorname{erf}(\infty) = 1, \quad \operatorname{erf}(-\infty) = -1 \quad (\text{A-9})$$

$$\operatorname{erfc}(0) = 1, \quad \operatorname{erfc}(\infty) = 0, \quad \operatorname{erfc}(-\infty) = 2 \quad (\text{A-10})$$

The differentiation relation is

$$\frac{d}{dz} i^n \operatorname{erfc}(z) = -i^{n-1} \operatorname{erfc}(z), \quad (\text{A-11})$$

$$(n = 0, 1, 2, \dots, \text{ and } i = \sqrt{-1})$$

The integral relations are

$$i^n \operatorname{erfc} z = \int_z^\infty i^{n-1} \operatorname{erfc} t \, dt, \quad (\text{A-12})$$

$$(n = 0, 1, 2, \dots).$$

$$i^{-1} \operatorname{erfc} z = \frac{2}{\sqrt{\pi}} e^{-z^2}, \quad i^0 \operatorname{erfc} z = \operatorname{erfc} z \quad (\text{A-13})$$

$$\int \operatorname{erf}(z) \, dz = z \operatorname{erf}(z) + \frac{1}{\sqrt{\pi}} e^{-z^2} + \text{const.} \quad (\text{A-14})$$

$$\int \operatorname{erfc}(z) \, dz = z \operatorname{erfc}(z) - \frac{1}{\sqrt{\pi}} e^{-z^2} + \text{const.} \quad (\text{A-15})$$

Other useful integrals are

$$2 \int \exp\{-(az^2 + 2bz + c)\} \, dz = \sqrt{\pi/a} \cdot \exp\{(b^2 - ac)/a\} \cdot \operatorname{erf}(\sqrt{a} z + b/\sqrt{a}) + \text{const.} \quad (\text{A-16})$$

$$2 \int_0^\infty \exp\{-(az^2 + 2bz + c)\} \, dz = \sqrt{\pi/a} \cdot \exp\{(b^2 - ac)/a\} \cdot \operatorname{erfc}(b/\sqrt{a}) \quad (\text{A-17})$$

$$a \int e^{az} \operatorname{erf}(bz) \, dz = e^{az} \operatorname{erf}(bz) - \exp(a^2/4b^2) \operatorname{erf}(bz - a/2b) + \text{const.} \quad (\text{A-18})$$

The values of the functions $\operatorname{erfc}(z)$ and $e^{z^2} \operatorname{erfc}(z)$ are shown in Table 2 for several values of z in the range $-13.19 \leq z \leq 13.19$.

REFERENCE

Abramowitz, M. and I. A. Stegun, 1965: Handbook of Mathematical Functions.
Dover Publications, Inc., New York, Chapter 7, 295-330.

TABLE 2

VALUES OF $\text{erfc}(z)$ and $e^{z^2} \cdot \text{erfc}(z)$
FOR SEVERAL VALUES OF z .

| Z | ERFC(Z) | EXP(Z**2)*ERFC(Z) |
|--------|-------------|-------------------|
| -13.17 | 0.20000E 01 | 0.72091E 76 |
| -10.00 | 0.20000E 01 | 0.53762E 44 |
| -7.00 | 0.20000E 01 | 0.38147E 22 |
| -5.00 | 0.20000E 01 | 0.14401E 12 |
| -3.00 | 0.20000E 01 | 0.16206E 05 |
| -2.00 | 0.19953E 01 | 0.10894E 03 |
| -1.50 | 0.19661E 01 | 0.18654E 02 |
| -1.00 | 0.18427E 01 | 0.50090E 01 |
| -0.50 | 0.15205E 01 | 0.19524E 01 |
| 0.0 | 0.10000E 01 | 0.10000E 01 |
| 0.25 | 0.72367E 00 | 0.77035E 00 |
| 0.50 | 0.47950E 00 | 0.61569E 00 |
| 0.75 | 0.28884E 00 | 0.50694E 00 |
| 1.00 | 0.15730E 00 | 0.42758E 00 |
| 1.25 | 0.77100E-01 | 0.36782E 00 |
| 1.50 | 0.33895E-01 | 0.32159E 00 |
| 1.75 | 0.13328E-01 | 0.28497E 00 |
| 2.00 | 0.46777E-02 | 0.25540E 00 |
| 3.00 | 0.22090E-04 | 0.17900E 00 |
| 4.00 | 0.15417E-07 | 0.13700E 00 |
| 6.00 | 0.21520E-16 | 0.92777E-01 |
| 8.00 | 0.11224E-28 | 0.69985E-01 |
| 10.00 | 0.20885E-44 | 0.56141E-01 |
| 12.00 | 0.13563E-63 | 0.46854E-01 |
| 13.17 | 0.11833E-76 | 0.42652E-01 |



APPENDIX B

SETTLING AND DEPOSITION VELOCITIES

For a monodisperse particulate cloud, the individual particles have a constant gravitational settling velocity. This terminal velocity is given by Stokes' equation (Fuchs, 1964):

$$W = \frac{d^2 g \rho}{18 \mu} \quad (\text{B-1})$$

where d is the diameter of the particle, g is acceleration due to gravity, ρ is density of particles, and μ is the dynamic viscosity of air. For $d > 100 \mu\text{m}$, the terminal fall velocity is sufficiently great that turbulence in the wake of the particle cannot be neglected, and the viscous drag force F_d on the particle is greater than given by the Stokes' law, $F_d = 3\pi d\mu W$. For a particle with $d = 400 \mu\text{m}$, the actual value of W is about one-third the value given by Eq. (B-1). Stokes' expression for the drag force describes the effects of collisions between air molecules and a particle, assuming air to be a continuum. This assumption is not valid for very small particles, since the mean free path between molecular collisions is comparable to the particle size; under these conditions "slippage" occurs, and the particles undergo Brownian motion and diffusion, which give a terminal velocity greater than that predicted by Eq. (B-1). A discussion of the slip correction factor for the Stokes' equation can be found in Fuchs (1964) and Cadle (1975).

The values for the terminal gravitational settling velocities for different particulate materials are given in a tabular form by Lapple (1961) based on particle diameter and Reynolds number. These values, which account for the deviations from Stokes' equation discussed above, are given for spherical particles with a specific gravity of 2.0 in air at 25°C and 1 atm. pressure. This table has been reprinted in Sheely et al (1969) and Stern (1976).

The dry deposition pollutant-removal mechanisms at the earth's surface include gravitational settling, turbulent and Brownian diffusion, chemical absorption, inertial impaction, thermal, and electrical effects. Some of the deposited particles may be re-released into the atmosphere by mechanical resuspension. Following the concept introduced by Chamberlain (1953), particle removal rates from a polluted atmosphere to the surface are usually described by dry deposition velocities which vary with particle size, surface properties (including surface roughness (z_o) and moisture), and meteorological conditions. The latter include wind speed and direction, friction velocity (u_x), and thermal stratification of the atmosphere. Deposition velocities for a wide variety of substances and surface and atmospheric conditions may be obtained directly from the literature (e.g., McMahon and Denison, 1979; Sehmel, 1980). Sehmel and Hodgson (1974) gave plots relating deposition velocity (V_d) to d , z_o , u_x , and the Monin-Obukhov stability length.

Considerable care needs to be exercised in choosing a representative deposition velocity since it is a function of many factors and can vary by two orders of magnitude for particles. Generally, V_d should be defined relative to the height above the surface at which the concentration measurement is made. The

particle deposition velocity is approximately a linear function of wind speed and friction velocity, and its minimum value occurs in the particle diameter range 0.1 - 1 μm .

In the trivial case of $W = V_d = 0$, settling and deposition effects are negligible. For very small particles ($d < 0.1 \mu\text{m}$), gravitational settling can be neglected, and dry deposition occurs primarily due to the nongravitational effects mentioned above. In this case, $W = 0$ and $V_d > 0$. For small particles ($d = 0.1 \sim 50 \mu\text{m}$), $0 < W < V_d$; deposition is enhanced here beyond that due to gravitational settling, primarily due to increased turbulent transfer resulting from surface roughness. For larger particles ($d > 50 \mu\text{m}$), it is generally assumed that $V_d = W > 0$, since gravitational settling is the dominant deposition mechanism. When $W > V_d > 0$, re-entrainment of the deposited particles from the surface back into the atmosphere is implied as, for example, in a dust storm. The first four sets of model parameters given above are widely used in atmospheric dispersion and deposition of particulate material. The deposition of gases is a special case of the particulate problem with $W = 0$. Thus, one has to carefully select the values of W and V_d for use in the model.

REFERENCES

- Cadle, R. D., 1975: The Measurement of Airborne Particles. John Wiley & Sons, New York, 342 pp.
- Chamberlain, A. C., 1953: Aspects of travel and deposition of aerosol and vapor clouds. A.E.R.E. Report H.P.-1261, Atomic Energy Research Estab.; Harwell, Berks., U.K., 32 pp.
- Fuchs, N. A., 1964: The Mechanics of Aerosols. The Macmillan Co., New York, 408 pp.
- Lapple, C. E., 1961: J. Stanford Res. Inst. 5, p. 95.
- McMahon, T. A., and P. J. Denison, 1979: Empirical atmospheric deposition parameters - a survey. Atmospheric Environment 13, 571-585.
- Sehmel, G. A., and W. H. Hodgson, 1974: Predicted dry deposition velocities. Atmosphere-Surface Exchange of Particulate and Gaseous Pollutants. Available as CONF-740921 from NTIS, Springfield, VA., 399-423.
- Sehmel, G. A., 1980: Particle and gas dry deposition: a review. Atmospheric Environment 14, 983-1011.
- Sheehy, J. P., W. C. Achinger, and R. A. Simon, 1969: Handbook of Air Pollution. Public Health Service Publication No. 999-AP-44, U.S. E.P.A., Research Triangle Park, N.C.
- Stern, A. C., 1976: Air Pollution. Academic Press, New York, Vol. I, 3rd ed., 715 pp.

APPENDIX C

PROPOSED FIELD STUDY

by

Bruce B. Hicks, Director

Atmospheric Turbulence and Diffusion Laboratory
National Oceanic and Atmospheric Administration
Oak Ridge, Tennessee 37830

APPENDIX C

PROPOSED FIELD STUDY

The limitations of surrogate-surface and deposition-vessel methods for evaluating dry deposition rates of airborne pollutants are well known. In response to their recognized inability to reproduce the fine-scale features of surfaces, a variety of alternative methods of measurement have been developed. In general, these have been applied in studies of specific pollutants for which specially accurate and/or rapid response sensors are available. The philosophy of these experiments is not to measure directly the long-term deposition flux, but instead to develop formulations suitable for evaluating average deposition rates from other, more easily obtained information, such as air concentrations, wind speed, and vegetation characteristics. Most studies of this kind have employed either the well-known gradient method, or the more complicated but potentially more accurate eddy-correlation technique. The former requires that concentration differences of the order of 1% be measured with accuracy; the latter requires that sensors respond with time constants faster than one second. In the case of airborne hydrocarbons and similar potentially hazardous materials, neither requirement is likely to be met. Therefore, we propose that a new method of inferring deposition fluxes from less-than-perfect sensors should be developed and used in exploratory field investigations on the deposition of toxic substances.

The essence of the method suggested is to extend measurements of fluxes which can be measured directly to the case of other quantities by comparing turbulent fluctuations in carefully-controlled frequency bands. All flux measurements would be referred back to a single easily measured quantity, the net radiation, R_N . Values of R_N are readily obtained by mounting a commercially-available net radiometer at a height a few meters above a selected surface. As in most studies of this kind, considerable care would be required in selecting the site to be used and in deploying the radiometer. For the present, the details of site selection can be summarized by stating the obvious requirements for as flat an area as possible, with a spatially homogeneous surface.

Incoming net radiation can be apportioned into sensible (H) and latent (LE) heat fluxes by any of a number of so-called Bowen ratio methods. Depending on the circumstances and on the accuracy required, it might be necessary to consider (and measure) the ground heat transfer G, in order to identify the sum of H and LE:

$$H + LE = R_N - G \quad (C-1)$$

If δT is a characteristic property of the (short-term, ~ 1 hour) temperature field in the surface boundary layer, and if δq is a corresponding humidity characteristic, then the Bowen ratio β can be expressed as

$$\beta \equiv H/LE = \rho c_p \delta T/L \delta q \quad (C-2)$$

where ρ is density of air, c_p is the specific heat of air at constant pressure,

and L is the latent heat of vaporization of water. (Here, δT will have units of $^{\circ}\text{C}$, and δq of g m^{-3}), Clearly, (C-1) and (C-2) allow us to evaluate H and LE as

$$H = \beta (R_N - G)/(1 + \beta) \quad (\text{C-3})$$

and

$$LE = (R_N - G)/(1 + \beta) \quad (\text{C-4})$$

If we have an analogous pollutant concentration characteristic, δC , then we can evaluate the pollutant flux F_c as

$$F_c = (\delta C / \delta T) \cdot (H / \rho c_p) \quad (\text{C-5})$$

As a further step, the appropriate deposition velocity can then be evaluated as

$$V_d \equiv F_c / C = (\delta C / C) \cdot (H / \rho c_p) \cdot (1 / \delta T) \quad (\text{C-6})$$

A little more manipulation of the algebra leads to an interesting form for V_d :

$$V_d = (\delta C / C) \cdot (R_N - G) / (\rho c_p \delta T + \rho L \delta q). \quad (\text{C-7})$$

Equation (C-7) offers considerable promise. In concept, it will permit us to evaluate V_d without any direct measurement of turbulent fluxes by either covariance or gradient methods. Instead, it relies on apportioning the incoming heat energy (R_N) by using some measure of the temperature and humidity conditions, and applying an identical measure of the pollutant concentration. Clearly, vertical differences over the same height interval would provide a sufficient

quantification of δT , δq , and δC . However, it is proposed here that a better measure is a relatively slow component of turbulence, for example at the frequency typical of the process of turbulent exchange (~ 20 seconds period).

In order to apply the method in practice, it is necessary to be sure that the amplitude of signals in the selected frequency range is not affected by noise, or else to quantify the noise component. To these ends, spectral analysis methods will be used, providing power spectral estimates as a function of frequency for each of T , q , and C . Figure C-1 demonstrates the sort of result that might be expected, and shows how an appropriate frequency band might be selected. It is critical that the effects of noise be properly accounted for, since otherwise spectral techniques will necessarily result in an overestimation of the corresponding deposition velocity.

There are a number of assumptions involved in the preceding analysis. All of them are important, but none are considered prohibiting. For example, in order to apply similar relationships for δT , δq , and δC , it is required that the corresponding sources and sinks should be coincident. While this requirement is obviously satisfied in many situations (e.g. over pasture, water, or tarmac), tests of the validity of the assumption will often be necessary (e.g. over forest). Suitable tests might involve the use of several measures of the indicators δT , δq , and δC , in different frequency bands for example.

The philosophy of this kind of experiment is similar to that employed in the interpretation of structure functions and high-frequency spectral data in many micrometeorological studies. It is conceded that the method is not norm-

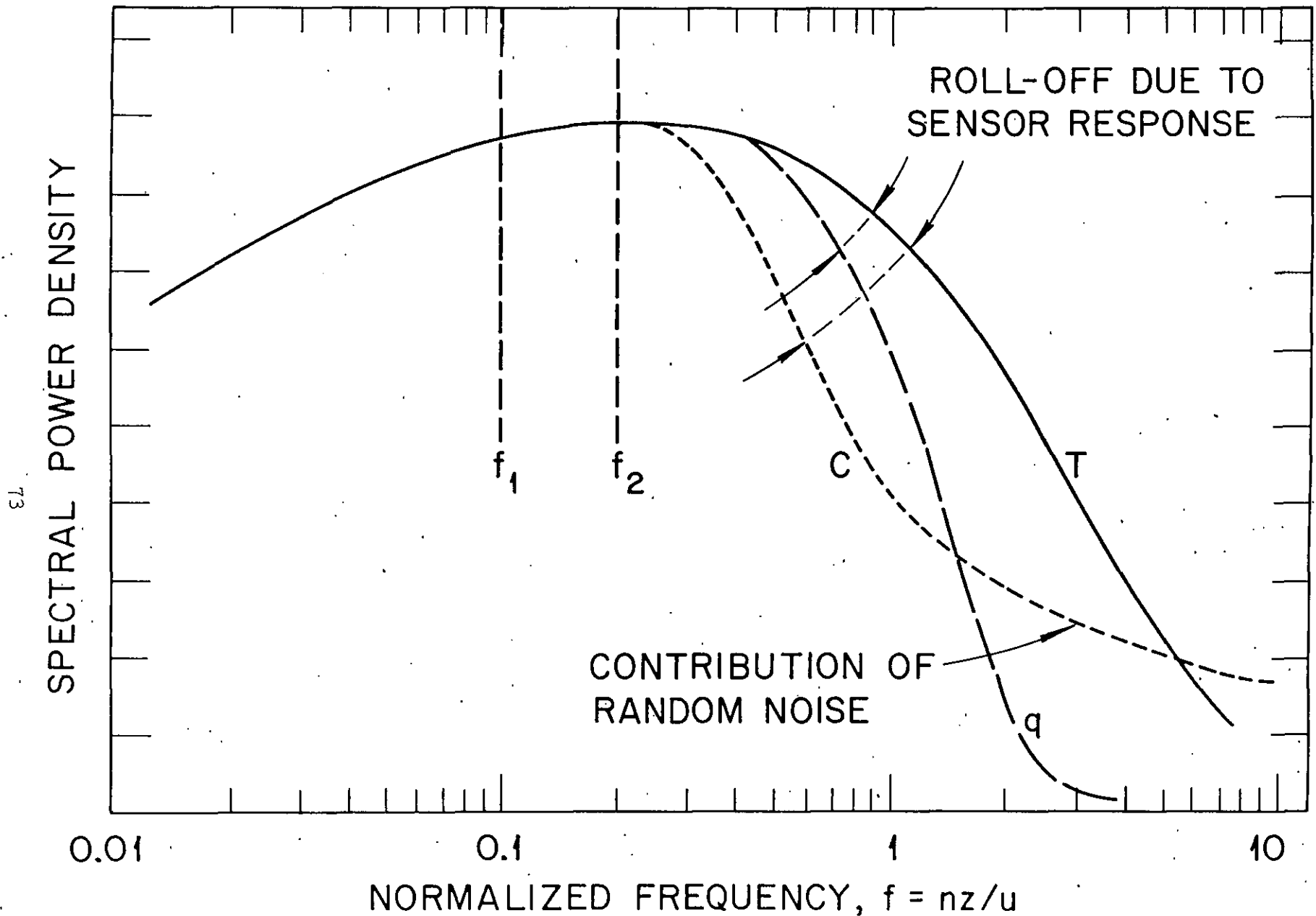


Figure C-1. Schematic representation of the effects of limited response of q and C sensors on power spectra, and of the effects of noise on the C -spectrum. The T -spectrum is assumed to be "pure". In this case, the frequency band $f_1 - f_2$ should be

ally precise; in the method outlined here, accuracy should be improved by relating all temperature, humidity, and pollutant quantities to a flux that is well-known -- the net radiation. In practice, neglecting the ground heat transfer (and other small terms such as heat storage and photosynthesis) should cause a relatively small error in daytime, probably less than 15%. A first-order correlation can be applied on the basis of flux-plate data; however the evaluation of $R_N - G$ that results then is still likely to be about $\pm 5\%$ in error.

A measure of the errors involved can be obtained by applying methods for the direct determination of the turbulent fluxes H and LE from the spectral properties δT and δq , using standard micrometeorological procedures (e.g., Hicks and Dyer, 1972). Comparison between these estimates of H and LE with values deduced by apportioning $R_N - G$ (as above) will provide an indication of the magnitude of errors that might arise if data were not subjected to the $R_N - G$ "control". Comparison with independent evaluations of H and LE, obtained by eddy correlation, would permit a direct evaluation of run-to-run error margins involved in the determinations of H and LE by apportioning $R_N - G$. When coupled with run-to-run variability statistics of all three turbulent fluxes, H, LE, and F_c , a defensible estimate of the errors involved in the determination of V_d can be derived.

Several field studies are proposed, firstly to develop and test the techniques described here, and secondly to apply them in studies of toxic pollutant deposition. A well-instrumented field site, suitable for the former purpose, is available at Oak Ridge, where ATDL maintains and operates a forest meteorology/micrometeorology field station in a deciduous forest. Later work will be

conducted at selected field sites where pollutant concentrations are sufficiently high to permit studies of this kind.

Since sensors of suitable sensitivity and specificity are not likely to be available immediately, it is intended to consider the deposition of toxic chemicals in groups, according to physical and chemical characteristics. Although obviously not an ideal approach, this method will permit the application of existing sensors of materials like hydrocarbon vapors in scoping studies that will potentially provide answers to questions about the importance of surface dry deposition as a sink for airborne material, and the route by which such material enters the terrestrial biosphere.

REFERENCE

- Hicks, B. B. and A. J. Dyer, 1972: The spectral density technique for the determination of eddy fluxes. Quart. J. Roy. Meteorol. Soc. 98, 838-844.